

Femtosecond inscription in silica glass

**Mykhaylo Dubov, Vladimir Mezentsev,
Jovana Petrovic, Tom Allsop,
Amos Martinez, Yicheng Lai, and Ian Bennion**

Photonics Research Group, Aston University
B4 7ET Birmingham, United Kingdom



Jürgen Dreher, Rainer Grauer

Ruhr-Universität-Bochum, Universitätsstrasse 150
D-44780 Bochum, Germany



Where we are

Google Maps - photonics research group aston university - Mozilla Firefox

File Edit View Go Bookmarks Tools Help

http://maps.google.co.uk/

Getting Started Latest Headlines Telediscount: low cos... DiskImage 1.0 Scree... leagal

Help

Google Maps UK BETA

Search

Search the map
[Find businesses](#)
[Get Directions](#)

Results 1 - 4 of about 4 for **photonics research group aston university**

Categories: [Conference Facilities & Services](#)

A [Conference Aston](#)
within Aston University, The Aston Triangle, Birmingham, B4 7ET
0121 359 7293
[Alumni@home](#)
... A Hitch Hiker's Guide to Optical Fibre Networks, Professor Stephen Ferguson, Photonics Market Strategy Manager, Marconi ...
[aston.ac.uk](#)

B [Aston Science Park](#)
Business & Innovation Centre, Love Lane, Birmingham, B7 4BJ
0121 250 3500
[Aston Science Park - Text O...](#)
... of the business incubation support, accessing a range of technology partnerships and the resources of **Photonics** Cluster (UK).
...
[astonsciencepark.co.uk](#)

C [Oxford Fiber Ltd](#)
Aston Science Park Love Lane, Birmingham, B7 4BJ
0121 250 3588

Map Satellite Hybrid

Birmingham

Bochum

200 mi
200 km

©2006 Google - Imagery ©2006 NASA, Map data ©2006 TeleAtlas - Terms of Use

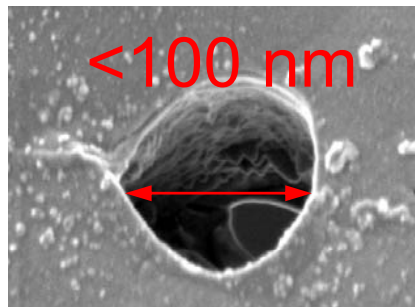
Done

Outline

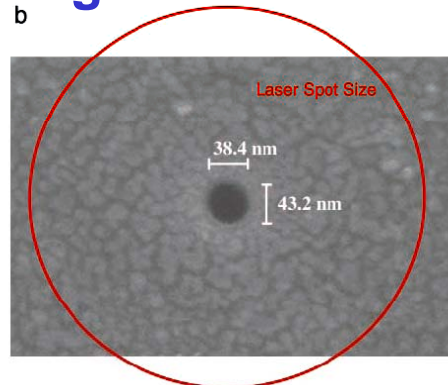
- ❑ Why femtosecond laser microprocessing?
- ❑ Modelling of femtosecond microfabrication
- ❑ Fiber-based photonic devices
 - Fibre Bragg Gratings
 - Long-Period Gratings
 - Short cavity Er:Yt fibre laser
- ❑ Planar structures
 - Waveguide fabrication
 - Sub-wavelength gratings
 - Experiments with high repetition rate system
- ❑ fs-assisted postprocessing (microfluidic applications)
- ❑ Future work

Femtosecond micro-fabrication/machining

Micromachining



Mazur et al, 2001



A.P. Joglekar, et al, PNAS-2004
Optics at critical intensity:
Applications to nanomorphing

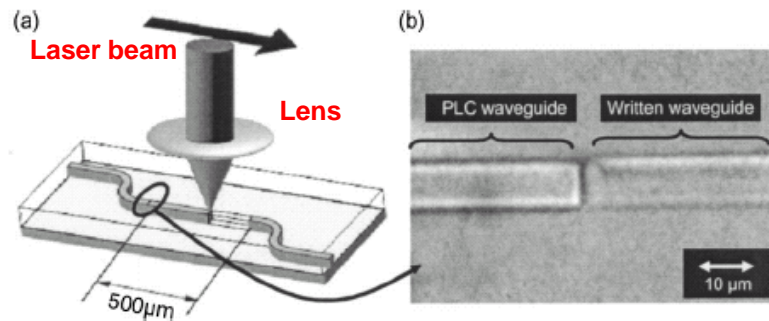


Fig. 5. (a) Schematic diagram of the waveguide connection in this experiment. (b) Image at the junction point of waveguide connection.

Nasu et al 2005, Planar Lightwave Circuits

Microfabrication



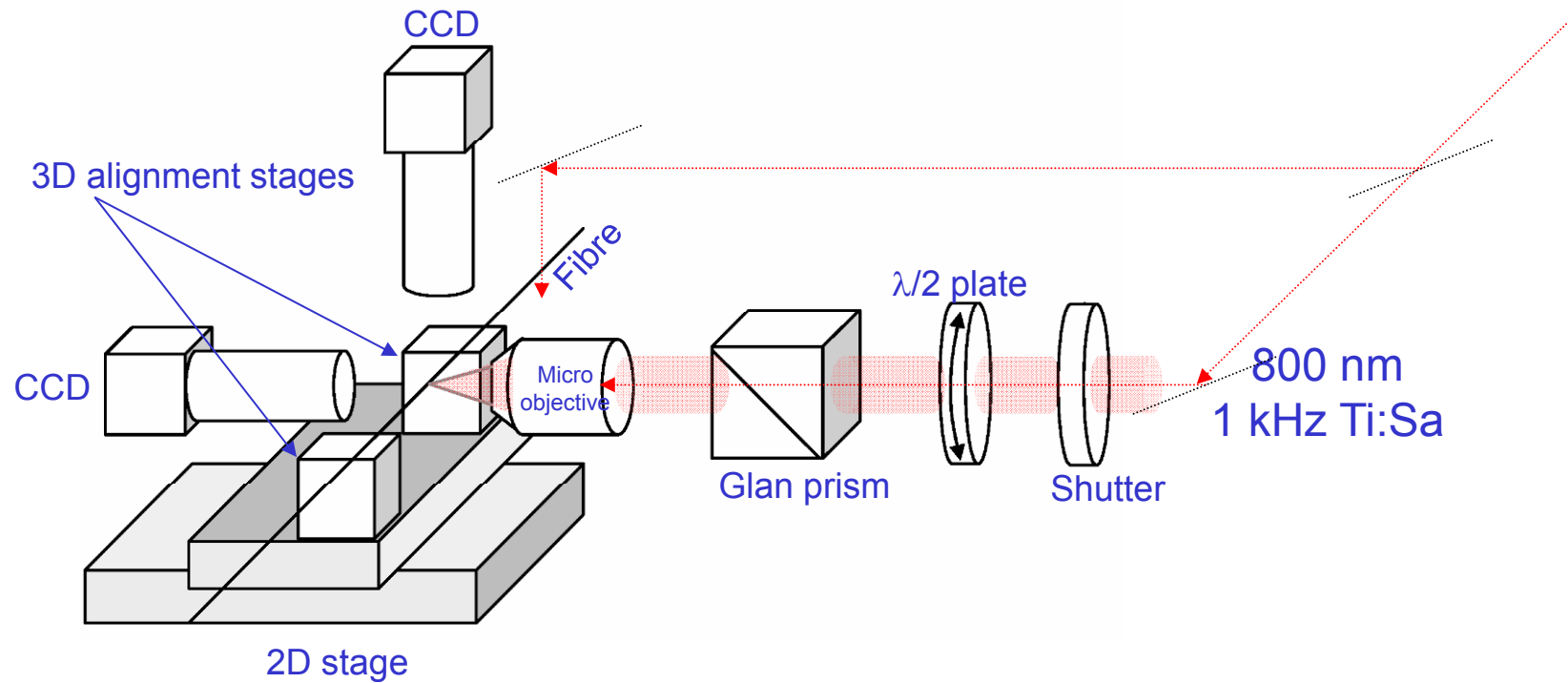
Fig. 1. (a) Schematic of the symmetric three-waveguide directional coupler. Waveguides are initially separated by $50\text{ }\mu\text{m}$ and by $5\text{ }\mu\text{m}$ in interaction region L . (b) Inverse gray-scale CCD image of the waveguide outputs shows a 43:28:29 power-splitting ratio between the guides.

Kowalevitz et al 2005,
3D couplers

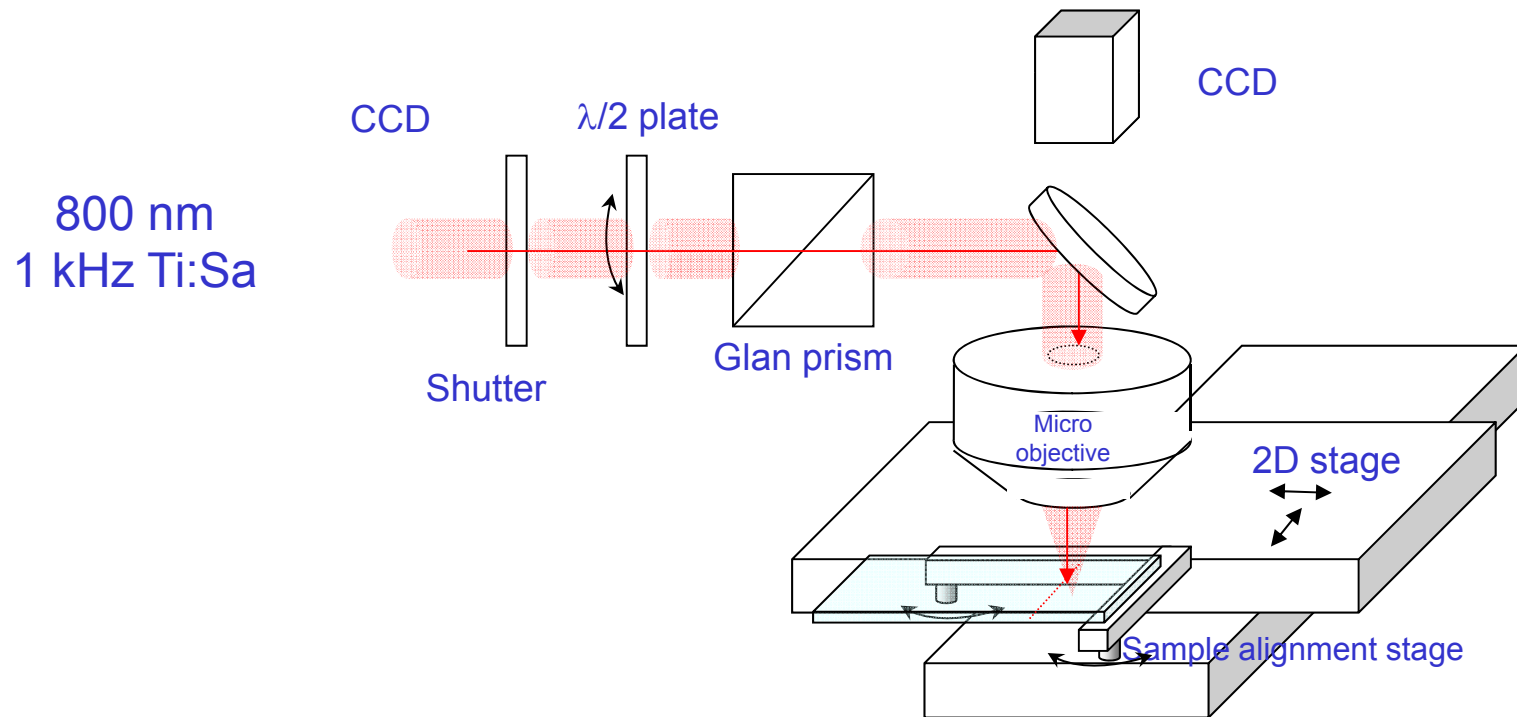


Aston 2004-2006

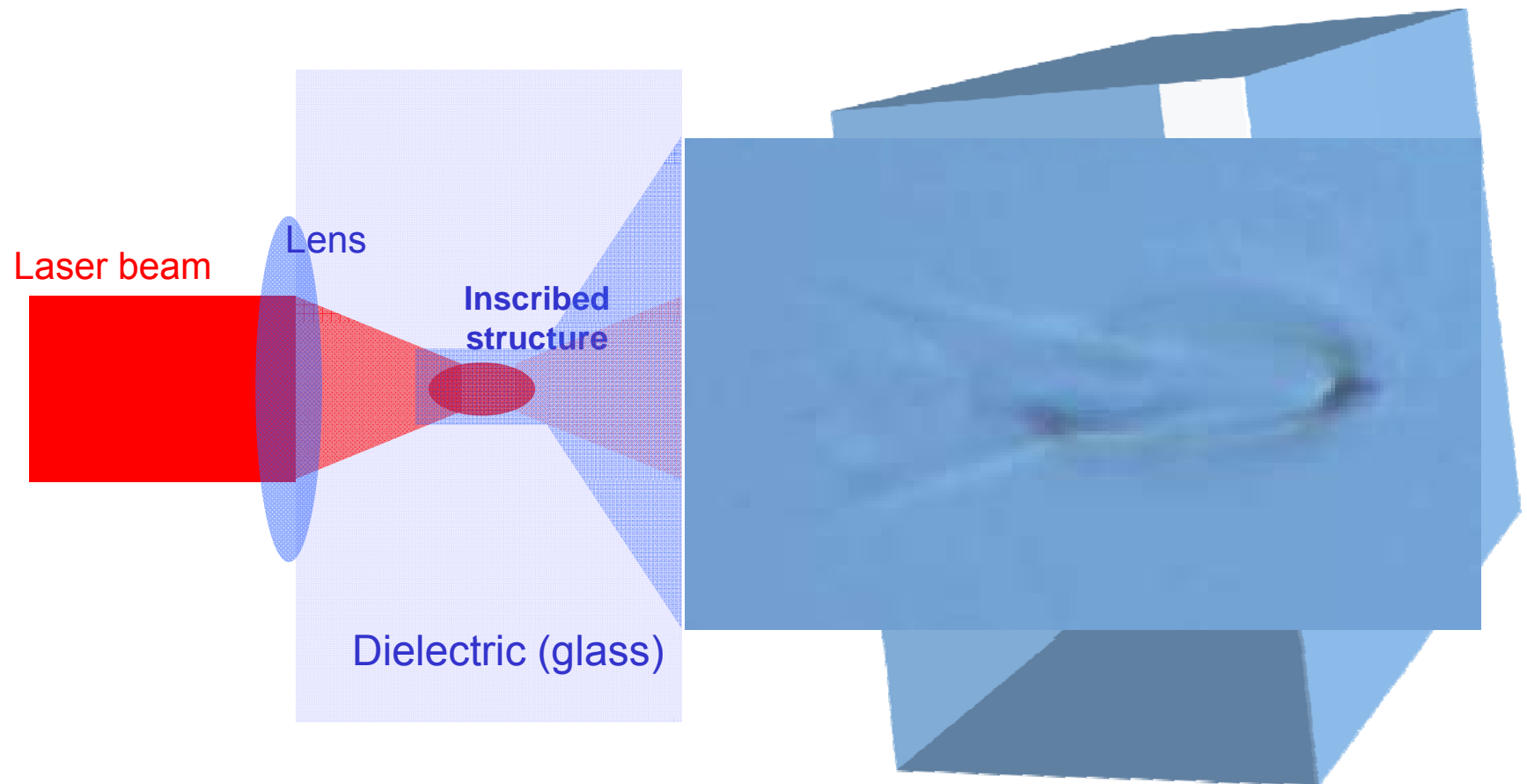
Experimental setup for fs microfabrication in fibres



Experimental setup for inscription in the bulk of the glass



Principle of laser microfabrication



Relatively low - energy femtosecond pulse may produce a lot of very localised damage

□ Pulse energy $E=1 \mu\text{J}$. What temperature can be achieved if all this energy is absorbed at focal volume $V=1 \mu\text{m}^3$?

□ $E=C_V\rho V\Delta T$

□ $C_V=0.75\times 10^3 \text{ J/kg/K}$

□ $\rho = 2.2\times 10^3 \text{ kg/m}^3$

□ Temperature is then estimated as **1,000,000 K (!)**

Larger, cigar shape volume **50,000 K**

Transparency **5,000 K**

Irradiation **2,000 K**

Why femtosecond?

Hengchang Guo, Hongbing Jiang, Ying Fang, J. Opt. A: Pure Appl. Opt. 6 (2004) 787–790

Inscription
region

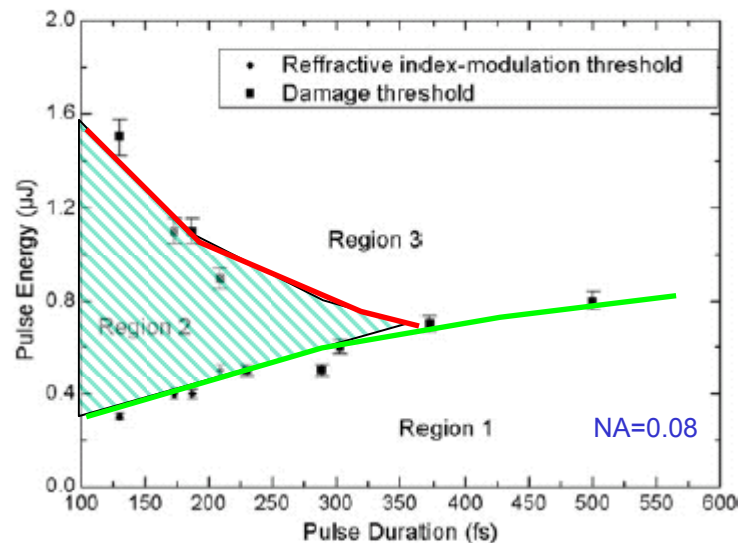


Figure 3. The dependence of the refractive index modulation threshold (♦) and damage threshold (■) on pulse duration with scan velocity of $10 \mu\text{m s}^{-1}$.

014104-3 Hnatovsky *et al.* Appl. Phys. Lett., 2005

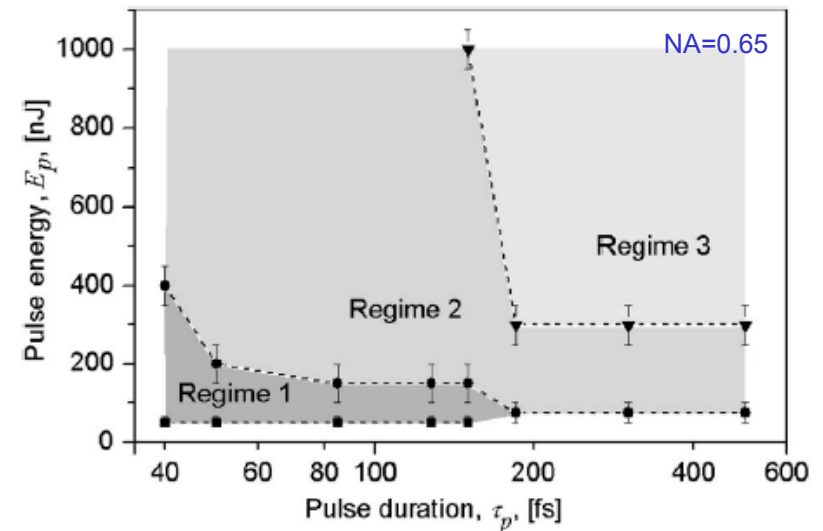


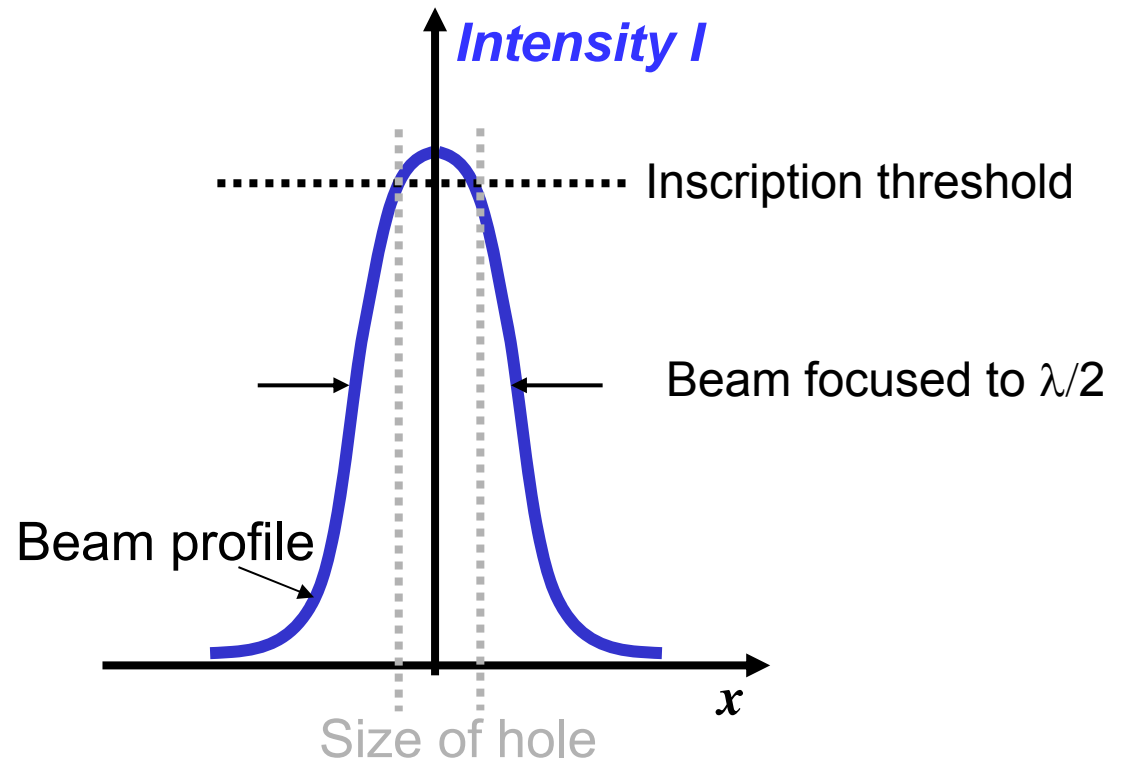
FIG. 2. Threshold pulse energies for different regimes of FLDM in fused silica. E_p 's between ■ and ● (regime 1) produce smooth modification, E_p 's between ● and ▼ (regime 2) produce nanogratings embedded into smooth modification, E_p 's above ▼ (regime 3) produce complex morphology comprising of disrupted regions, nanogratings, and smooth modification.

Sub-wavelength inscription

Naive observation:

Inscription is an irreversible change of refractive index when the light intensity exceeds certain threshold:

$$\Delta n \sim I - I_{th}$$



Careful control of the intensity can result in a very small structure, e.g., holes as small as ~40 nm have been created.

Experimentally determined inscription threshold for fused silica $I_{th} = 10 \div 30 \text{ TW/cm}^2$

Outline

- Why femtosecond laser microprocessing?
- Modelling of femtosecond microfabrication
- Fiber-based photonic devices
 - Fibre Bragg Gratings
 - Long-Period Gratings
 - Short cavity Er:Yt fibre laser
- Planar structures
 - Waveguide fabrication
 - Sub-wavelength gratings
 - Experiments with high repetition rate system
- fs-assisted postprocessing (microfluidic applications)
- Future work

Model (simplified as in [Feng et al., 1997])

**Non-Linear Schrödinger Equation
for envelope amplitude of electric field**

$$iE_z + \frac{1}{2k} \nabla_{\perp}^2 E + k_0 n_2 |E|^2 E = \frac{k''}{2} E_{tt} -$$

$$- \frac{i\sigma}{2} (1 + i\omega\tau) \rho E$$

Plasma Absorption
and Defocusing

$$- \frac{i\beta^{(K)}}{2} |E|^{2K-2} E$$

Multi-Photon Absorption

Balance rate equation for plasma density

$$\rho_t = \frac{1}{n_b^2} \frac{\sigma}{E_g} \rho |E|^2 + \frac{\beta^{(K)}}{K\hbar\omega} |E|^{2K}$$

Avalanche
ionization

Physical parameters [Tsortakis et. al, 2001] (fused silica, laser wavelength 800 nm)

$$k'' = 361 \text{ fs}^2/\text{cm} - \text{GVD coefficient}$$

$$n_2 = 3.2 \times 10^{-16} \text{ cm}^2/\text{W} - \text{nonlinear refraction index}$$

$$\sigma = 2.78 \times 10^{-18} \text{ cm}^2 - \text{inverse Bremsstrahlung cross-section}$$

$$\tau = 1 - \text{fs electron relaxation time}$$

$$\beta^{(K)} = \hbar \omega \sigma_K \rho_{at} - \text{MPA coefficient } (K=5)$$

$$\sigma_K = 1.3 \times 10^{-55} \text{ cm}^{2K}/\text{W}^K/\text{s}$$

$$E_g = 7.5 \text{ eV} - \text{ionization energy}$$

Physical parameters, cont.

$\rho_{at} = 2.1 \times 10^{22} \text{ cm}^{-3}$ – material concentration

$\rho_{BD} = 1.7 \times 10^{21} \text{ cm}^{-3}$ – breakdown density

$$I_{MPA} = \left(\frac{K \hbar \omega \rho_{BD}}{t_p \beta^{(K)}} \right)^{1/K} = 2.5 \times 10^{13} \text{ W/cm}^2 \text{ – naturally defined intensity threshold for MPA}$$

$$\rho_t = \frac{1}{n_b^2} \frac{\sigma}{E_g} \rho |E|^2 + \frac{\rho_{BD}}{t_p} \left| \frac{I}{I_{MPA}} \right|^K$$

It's seen that ionization kicks off when intensity exceeds the threshold I_{MPA}

Initial condition used in this presentation

Prefocused Gaussian pulse

$$E = \sqrt{\frac{2P_{in}}{\pi r_0^2}} \exp\left(-\frac{r^2}{r_0^2} - \frac{ikr^2}{2f} - \frac{t^2}{t_p^2}\right)$$

P_{in} – input power

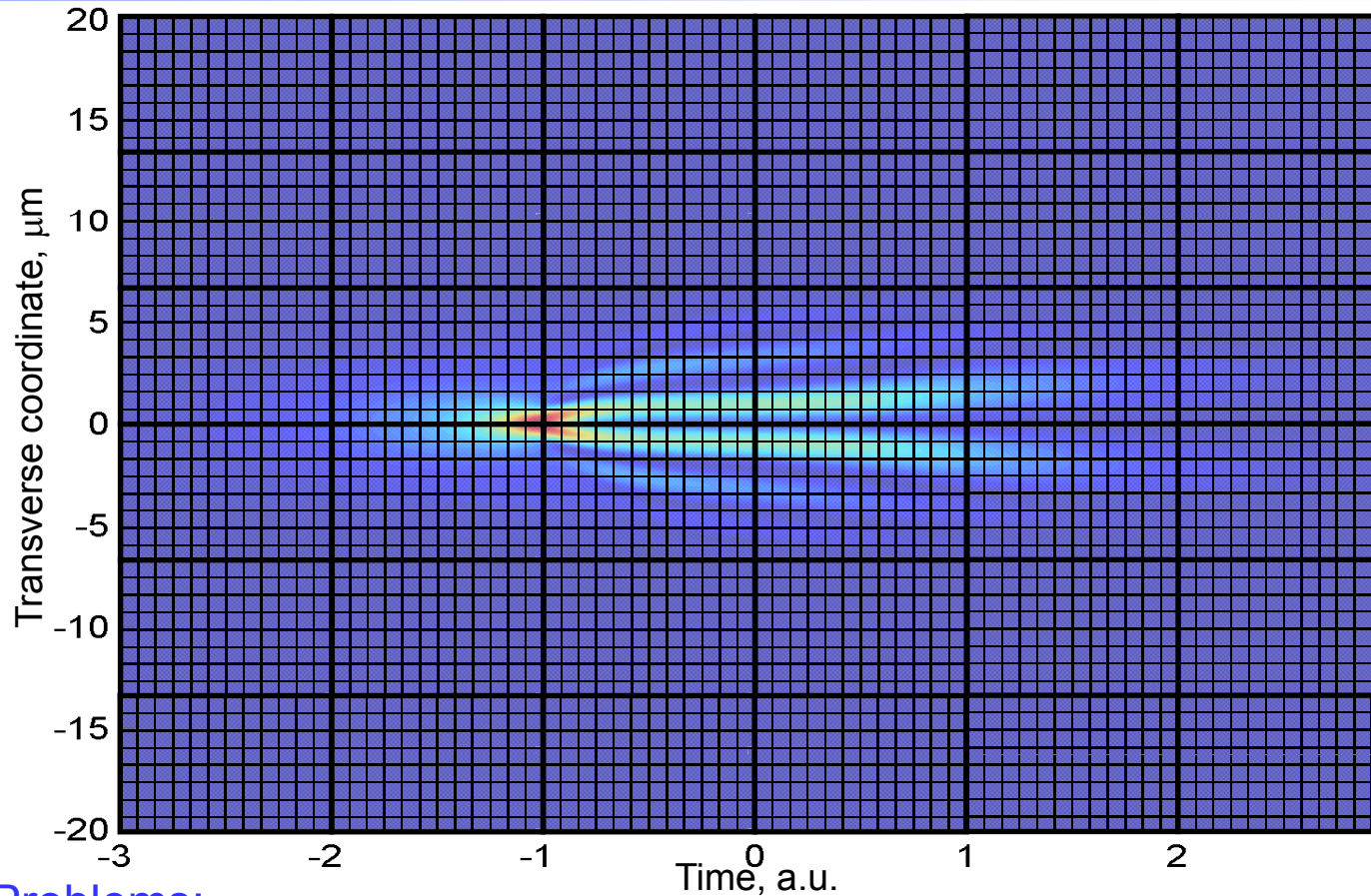
$r_0 = 2$ mm

$f = 40$ mm – lens focus distance

$t_p = 60$ fs

$P_{in} = \lambda^2 / 2\pi n n_2 \sim \mathbf{2.3\ MW}$ – critical power for self-focusing

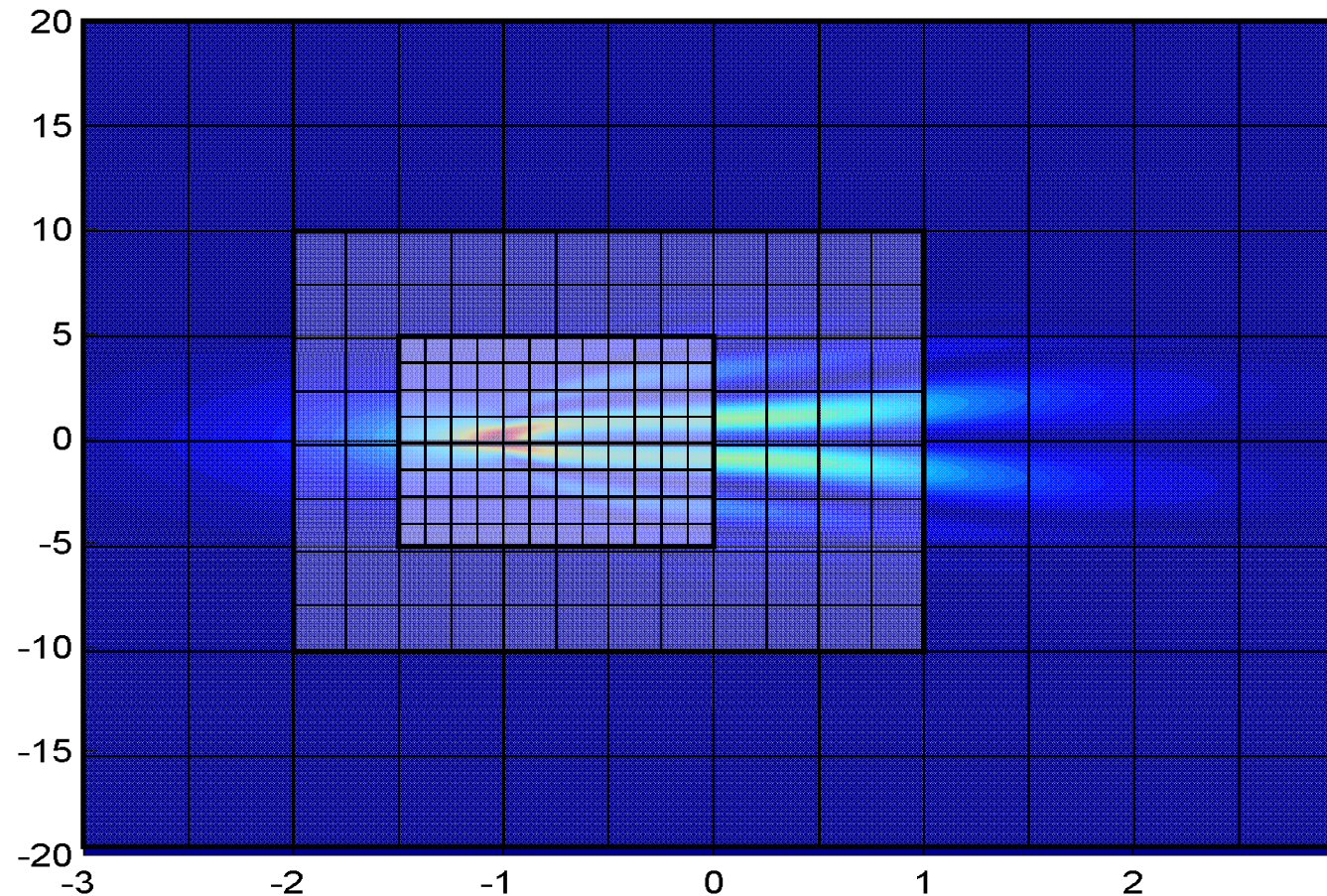
Numerical challenge



❑ Problems:

- Fine spatio-temporal features require fine resolution, hence, uniform meshing leads to over-resolution of smooth domains ☹
- Huge waste of CPU time, RAM, disk space ☹
- Properly resolved 3D run is impossible to complete in few weeks ☹

Adaptive mesh refinement

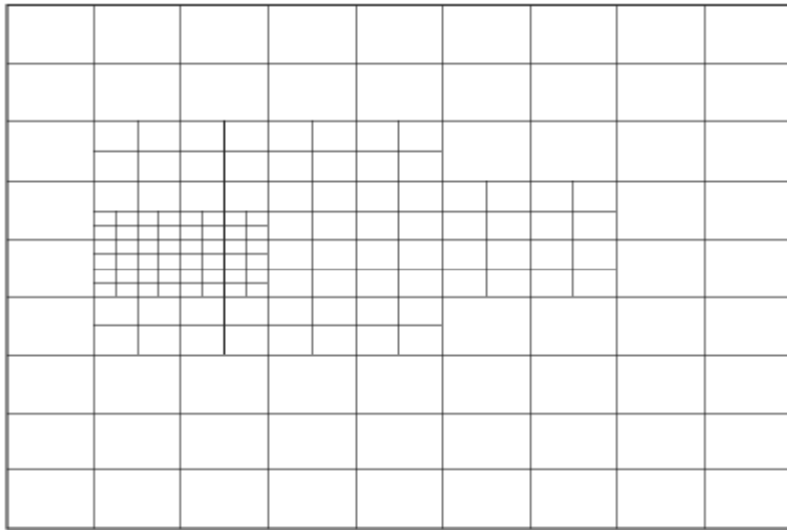


Principle: dynamically create adaptively adjustable hierarchy of meshes to resolve finest details (**refining**).

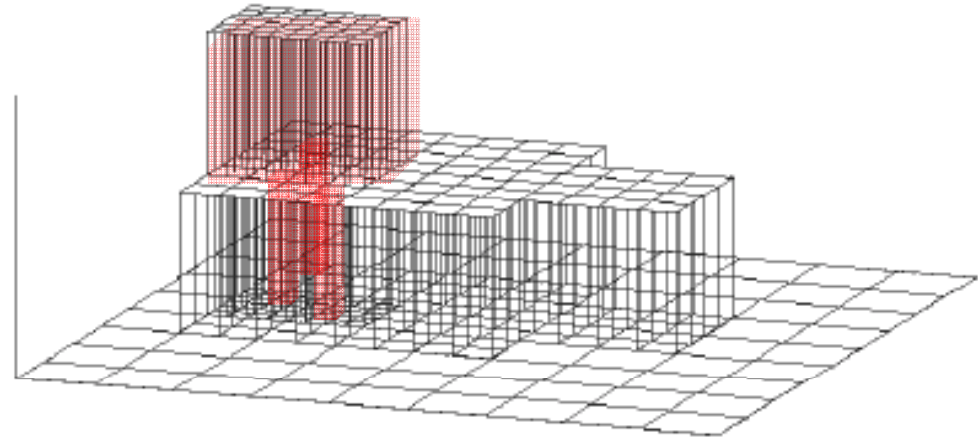
Fine meshes are removed when fine pattern disappears (**coarsening**).

Effective resolution in present work is up to **16384³ (!)**

Adaptive Refinement



Adaptively refined grids



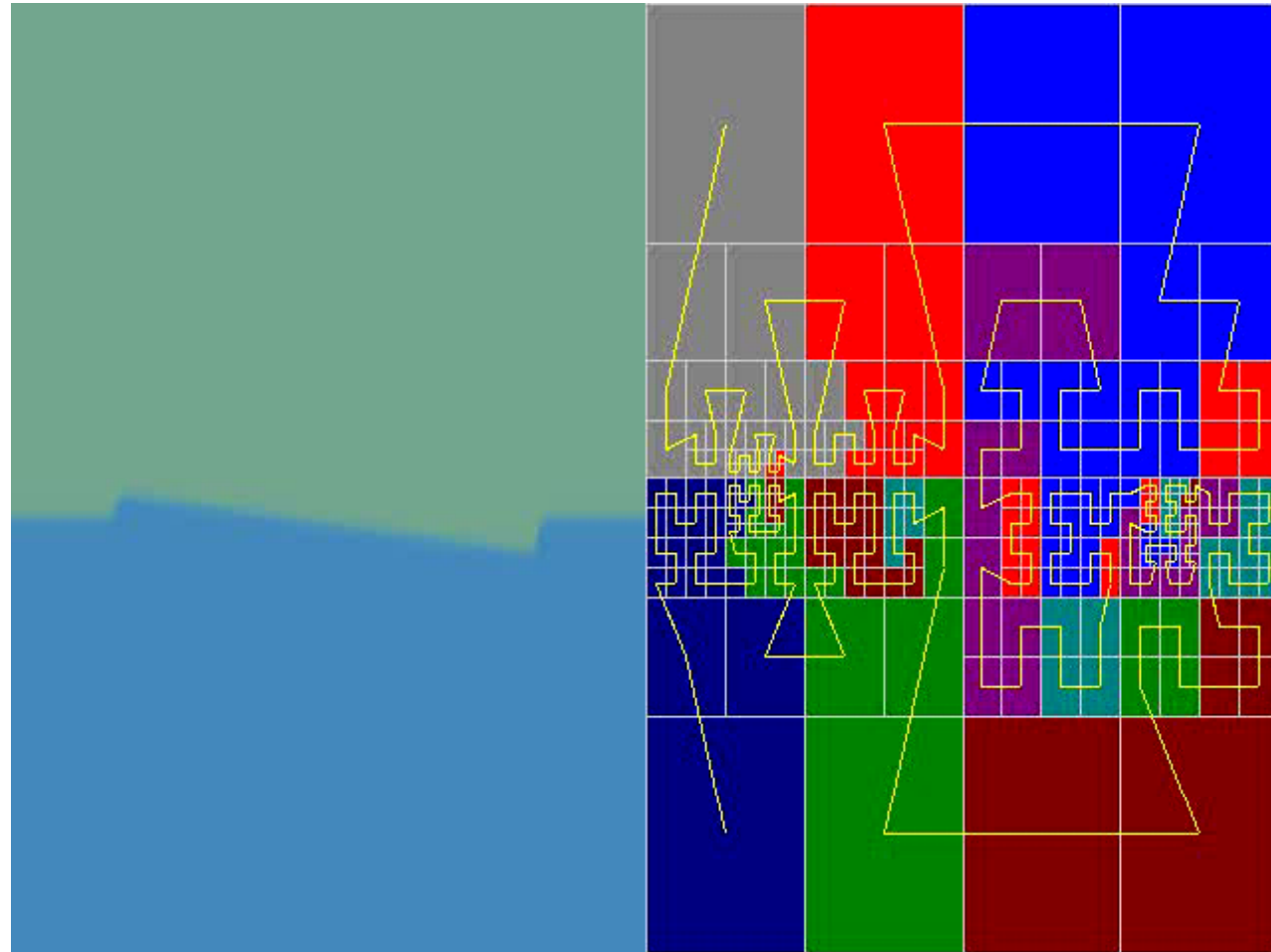
Hierarchy of grids – grids are on different levels of hierarchy

Liquid interface Instability

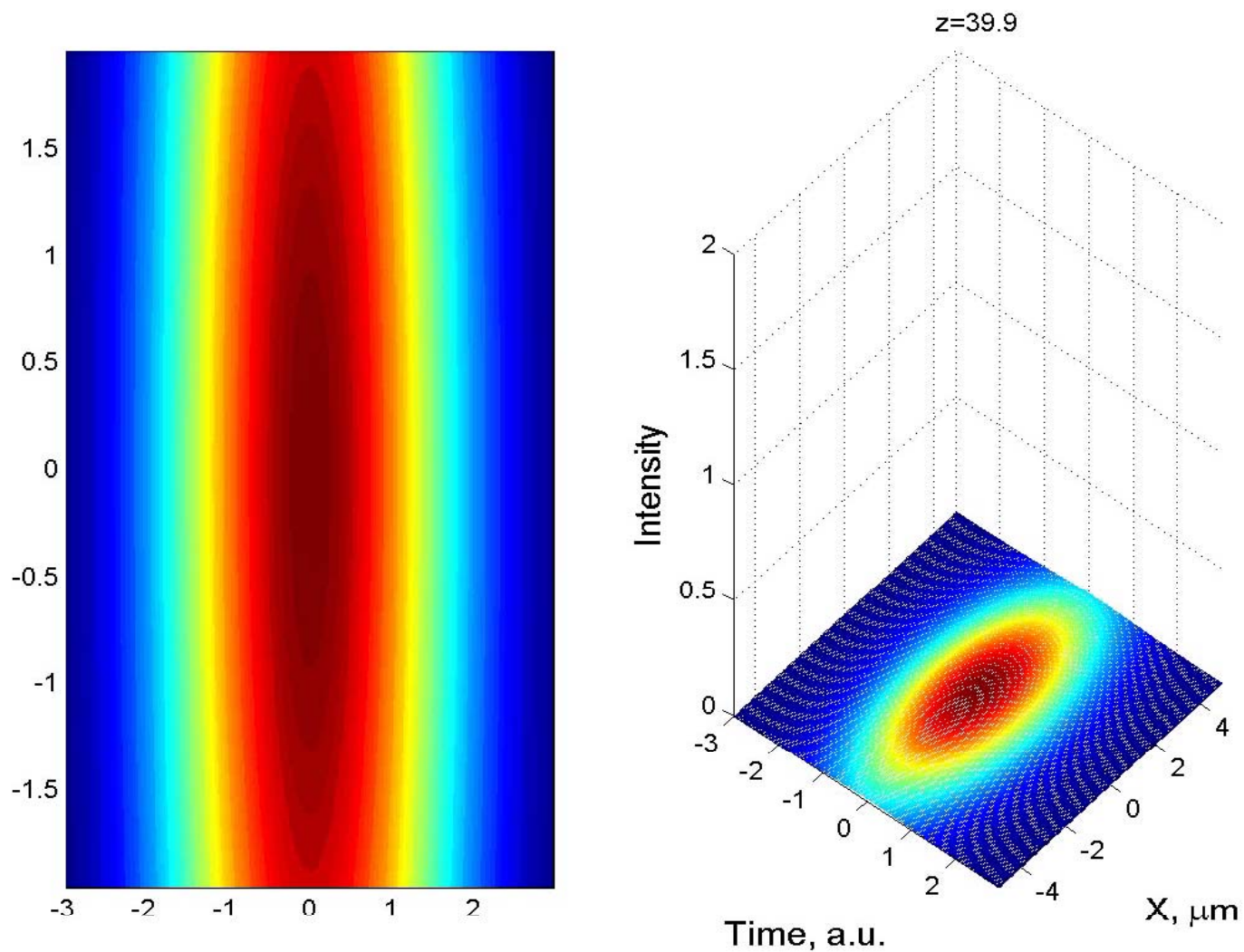
Jürgen Dreher,
Rainer Grauer,
2004



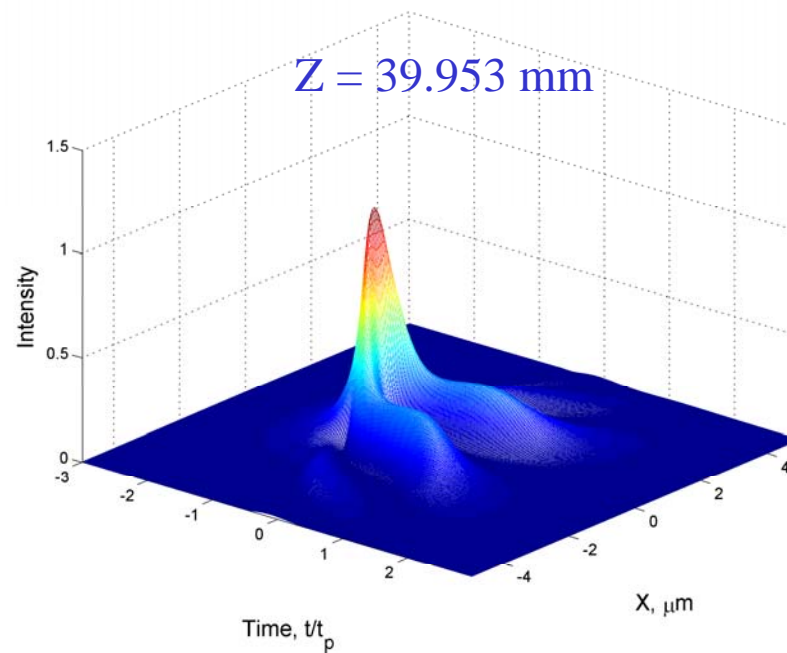
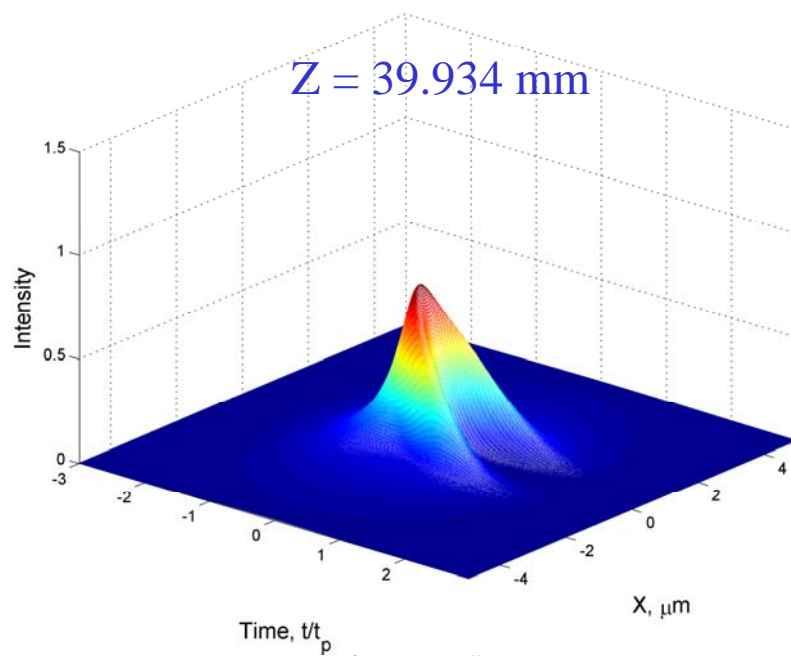
Ruhr-Universität-
Bochum, UniversitätsStr.
150,
D-44780
Bochum
Germany



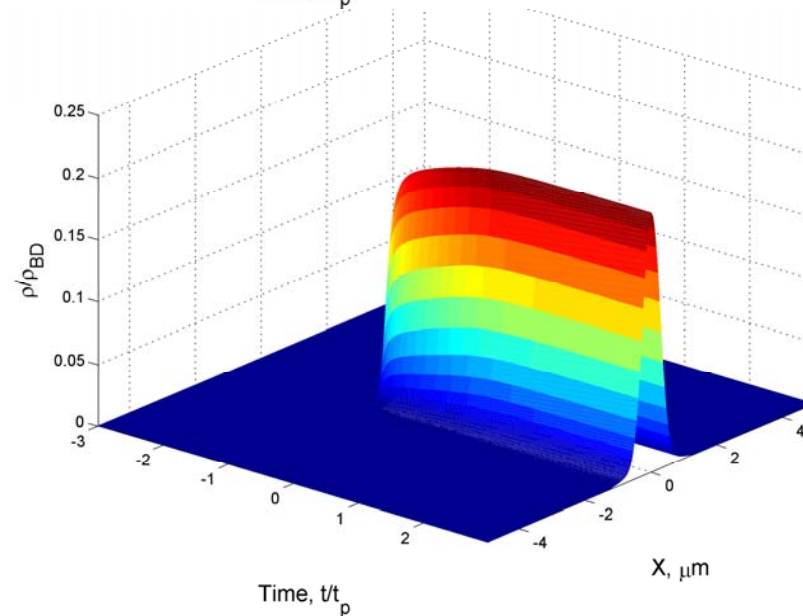
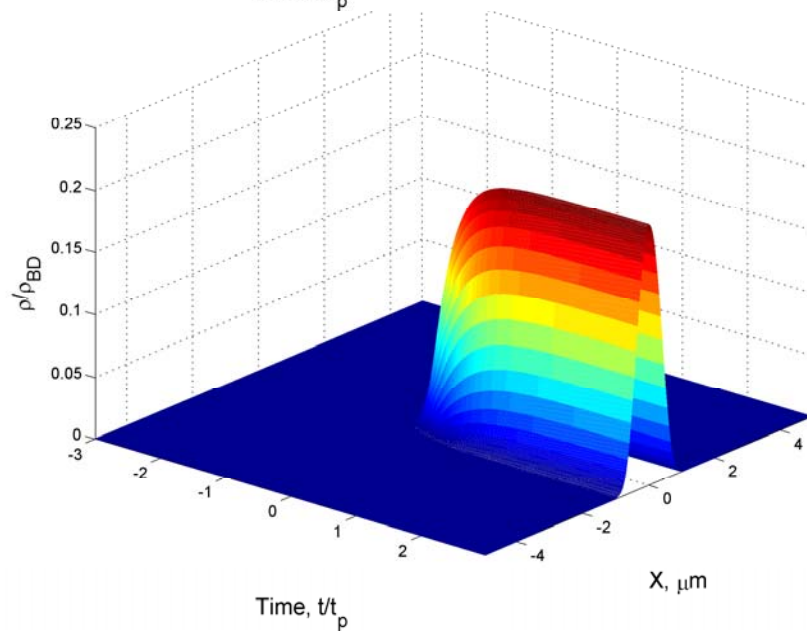
Spatio-temporal light dynamics



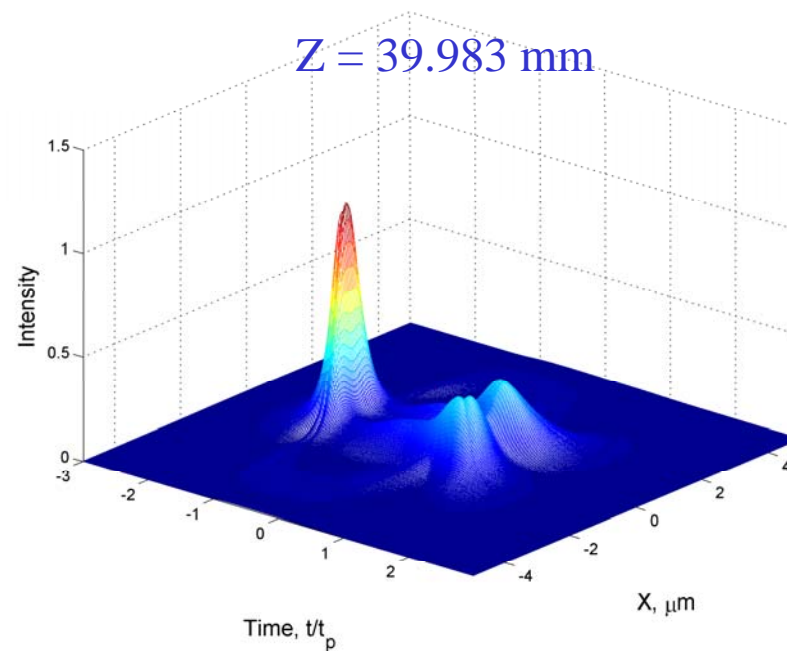
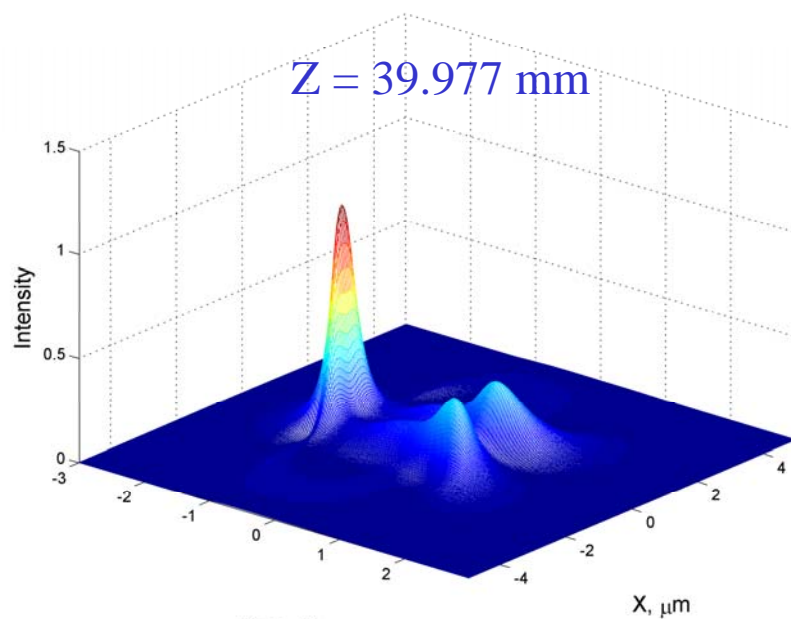
Intensity/ I_{MPA}



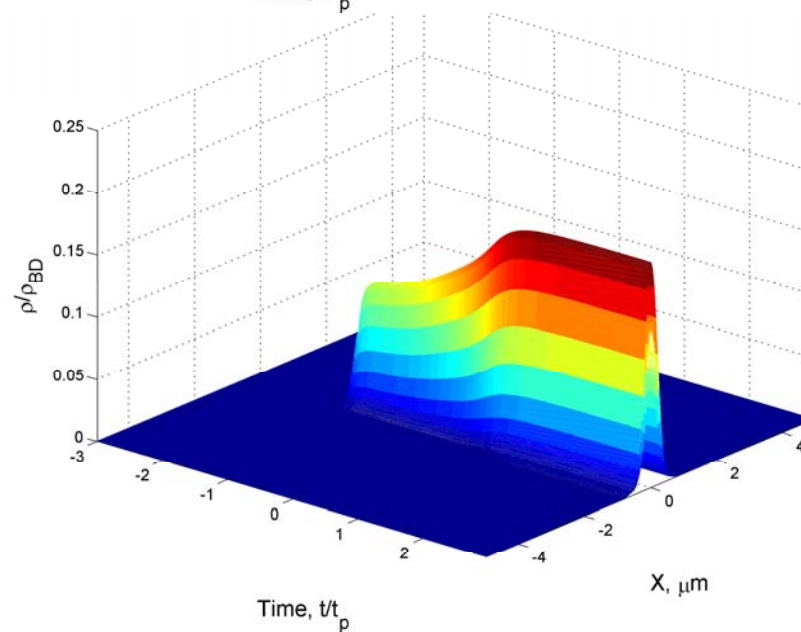
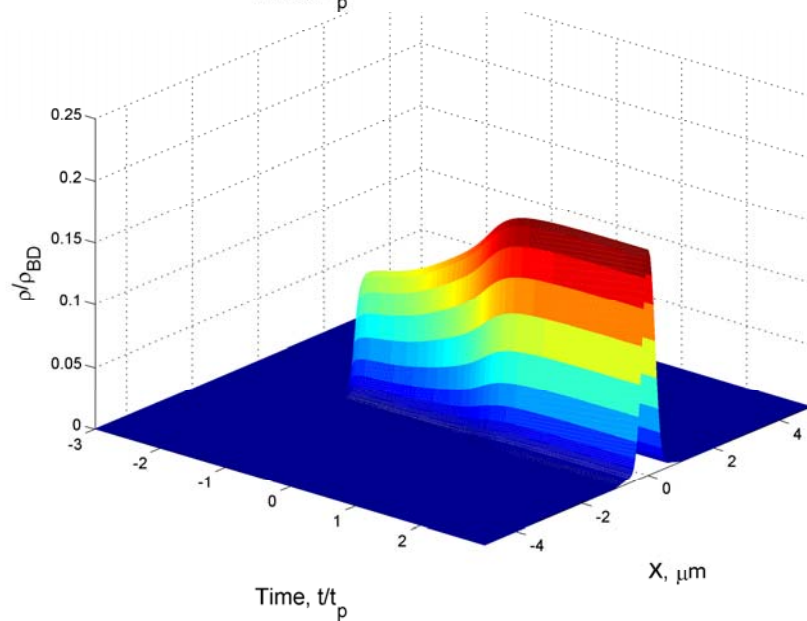
Plasma concentration



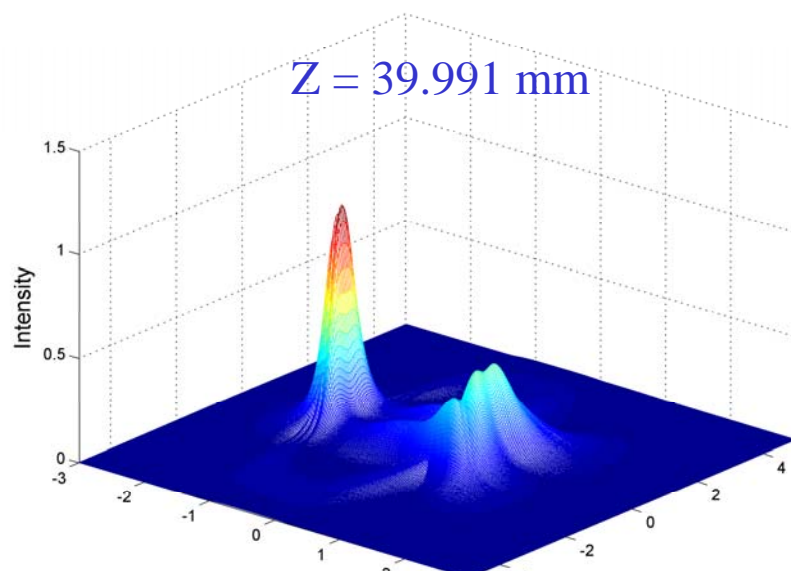
Intensity/ I_{MPA}



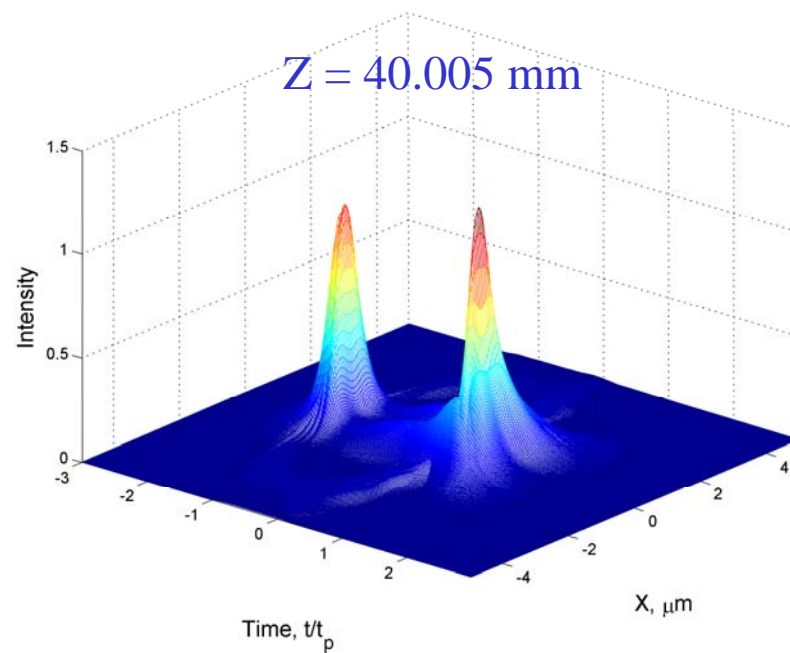
Plasma concentration



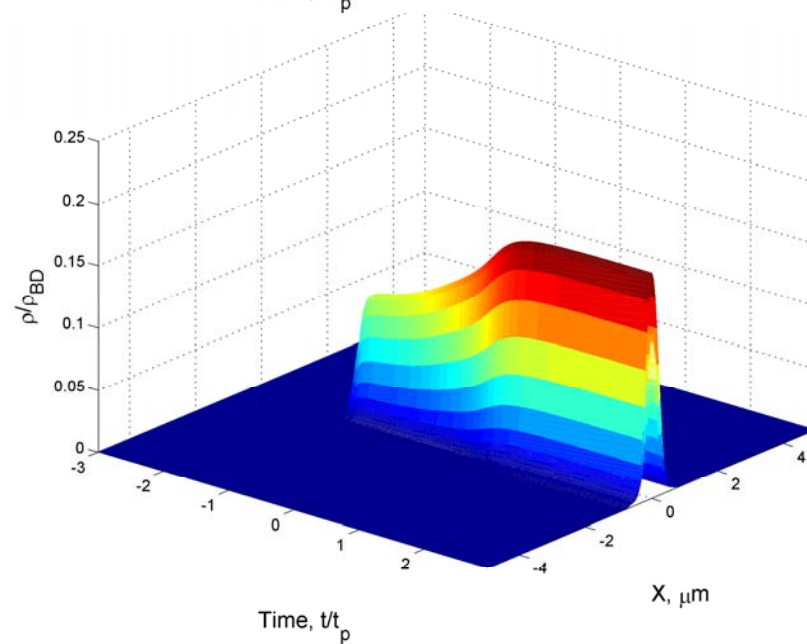
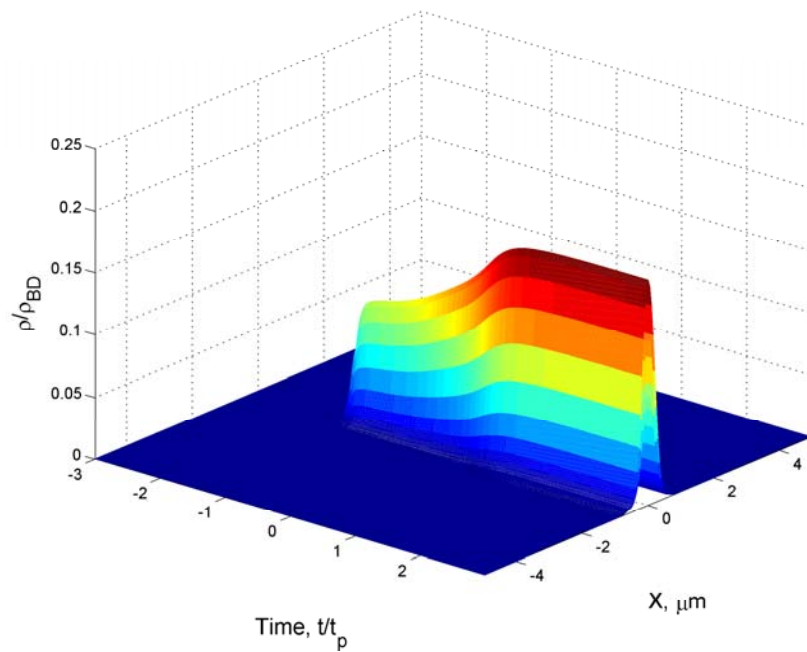
Intensity/ I_{MPA}



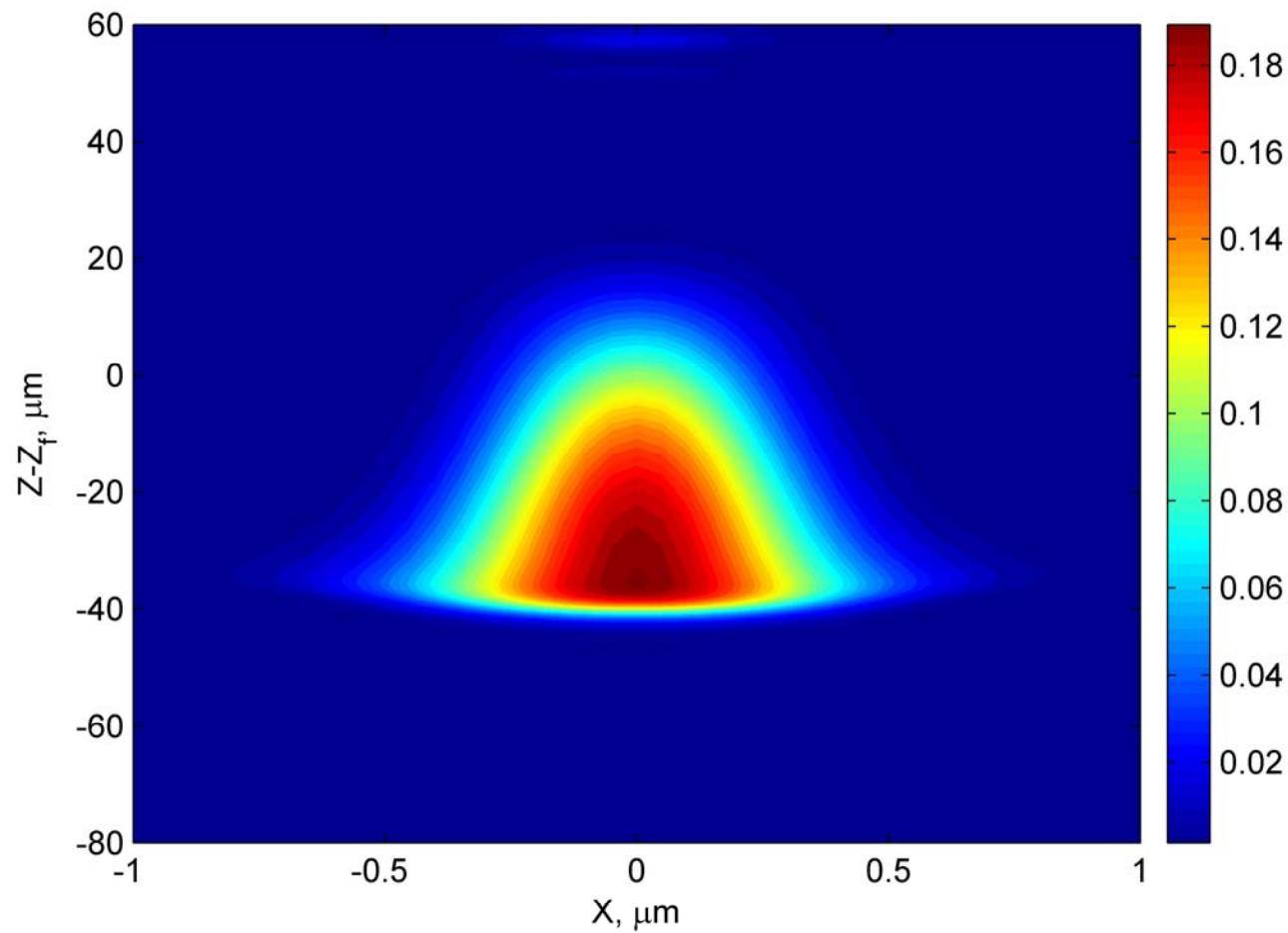
$Z = 40.005 \text{ mm}$



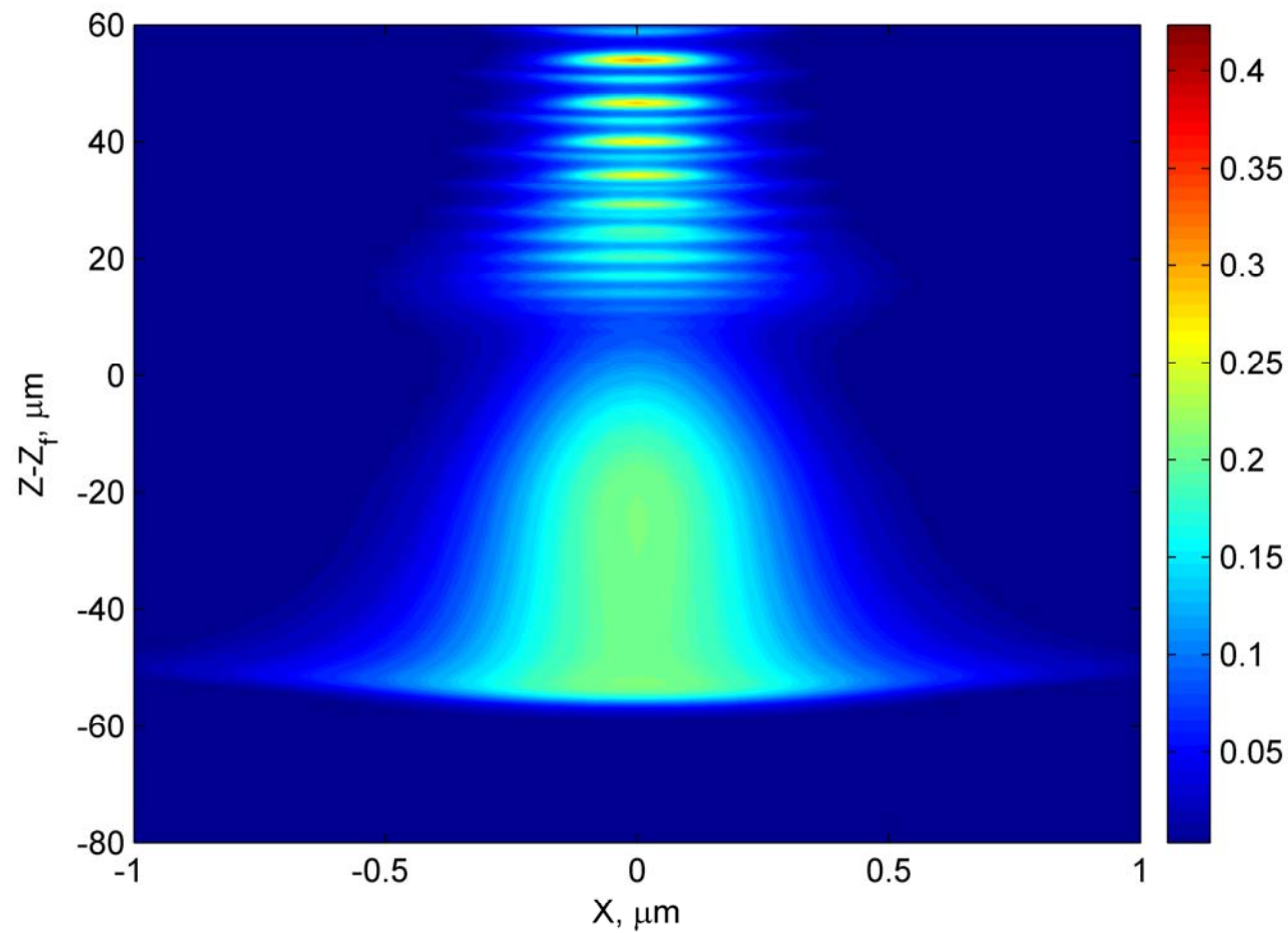
Plasma concentration



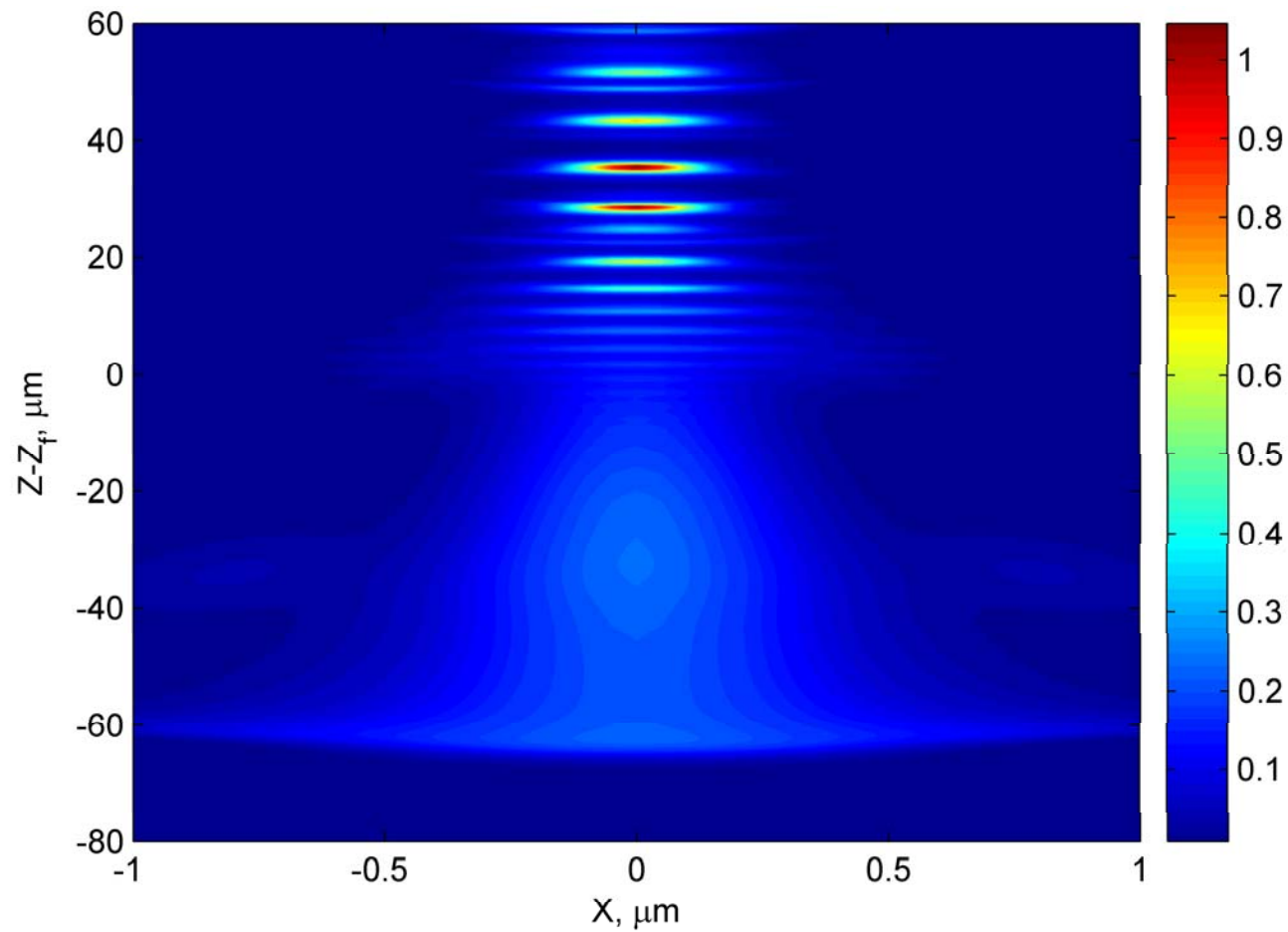
Plasma profile for subcritical power $P = 0.7 P_{cr}$



Plasma profile for critical power $P = 1.05 P_{cr}$

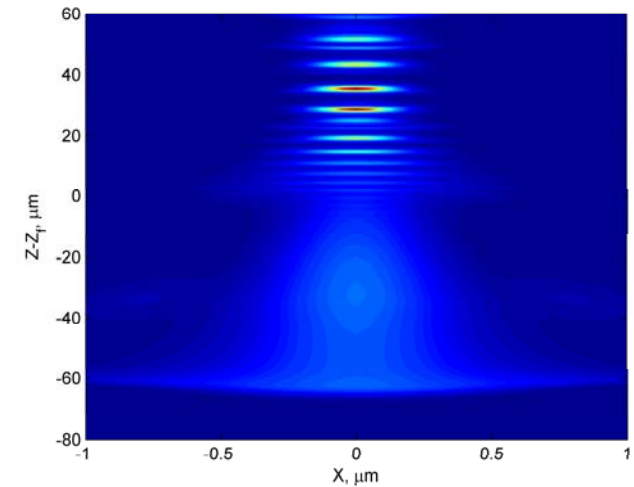
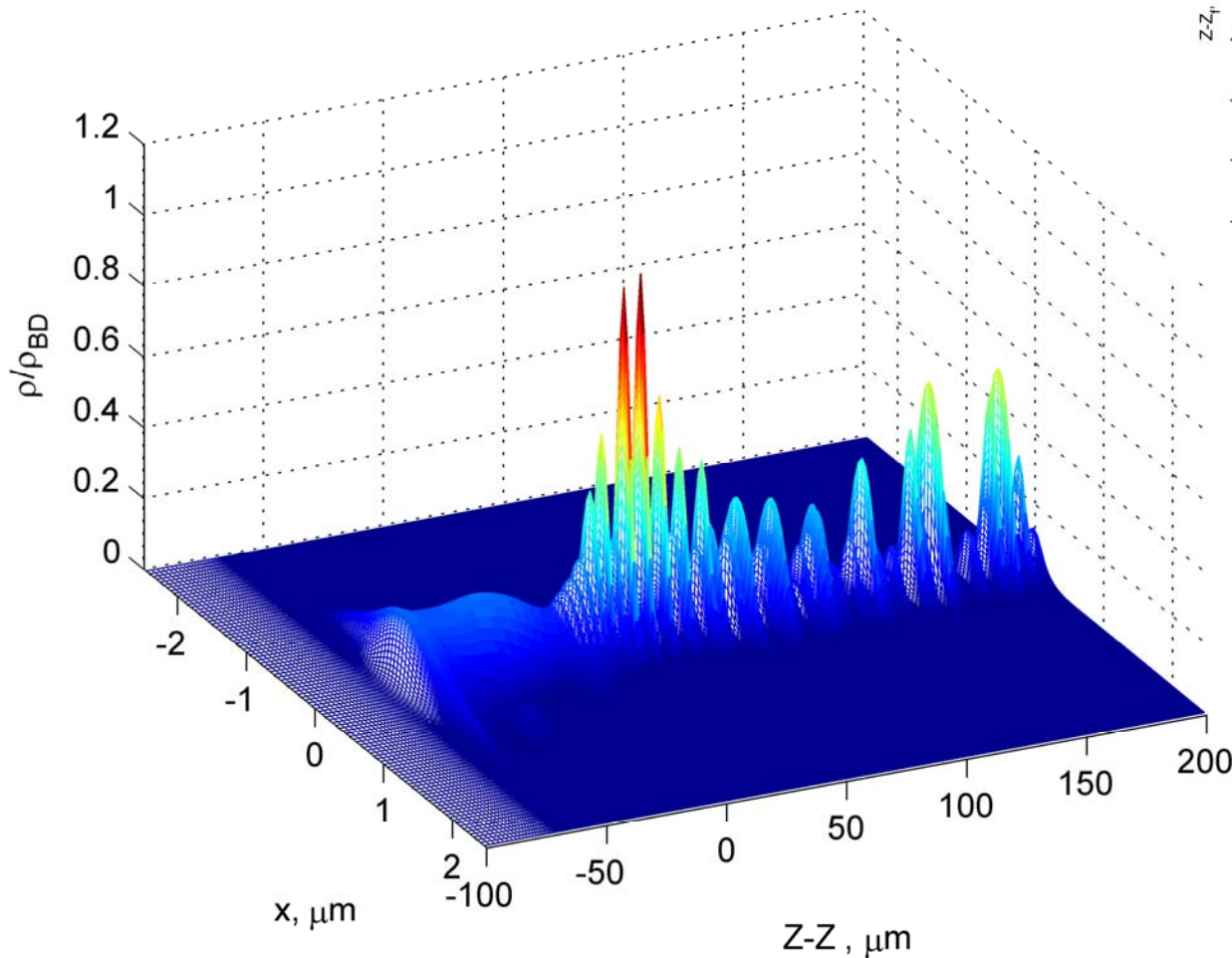


Plasma profile for supercritical power $P = 1.8 P_{cr}$



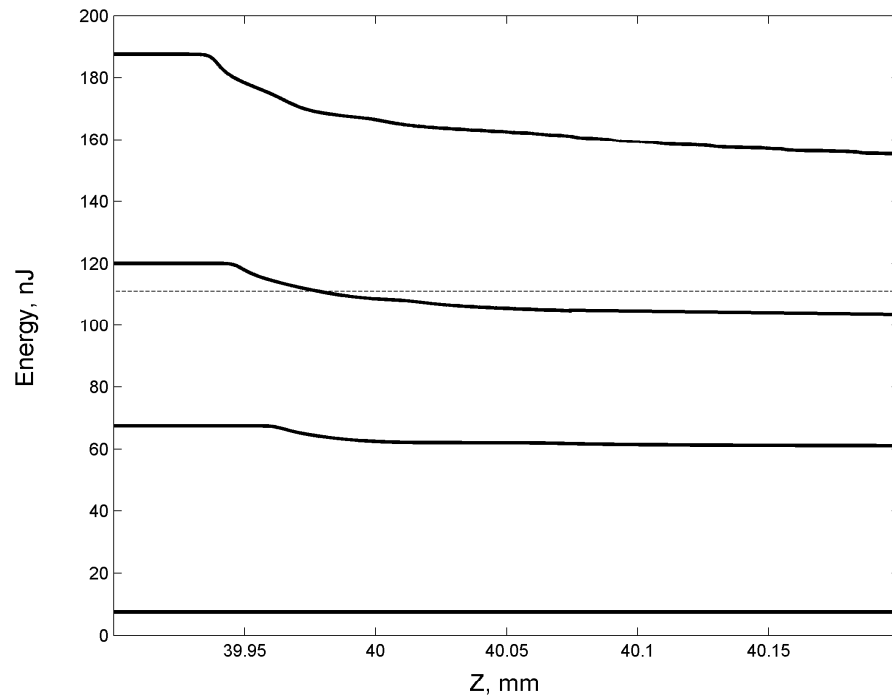
Plasma concentration profile

Supercritical case $P = 1.8 P_{cr}$

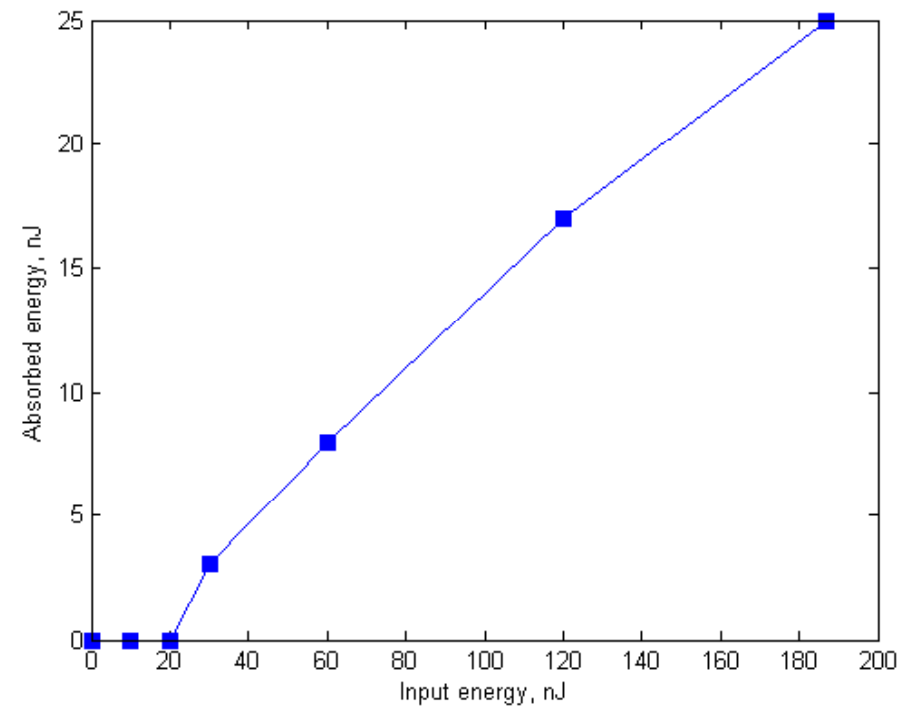


Slices of plasma are formed during the relaxation of the self-focusing beam. Self-focusing is arrested by MPA

Inscription threshold for Energy



Energy evolution



Absorbed energy vs input energy

Comparison with experiment

Single shot (supercritical power)

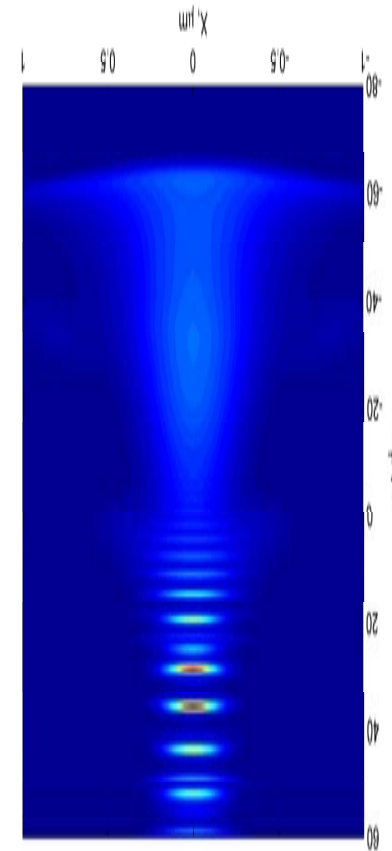


Petrovic, 2006



Dubov, 2006

Experiment



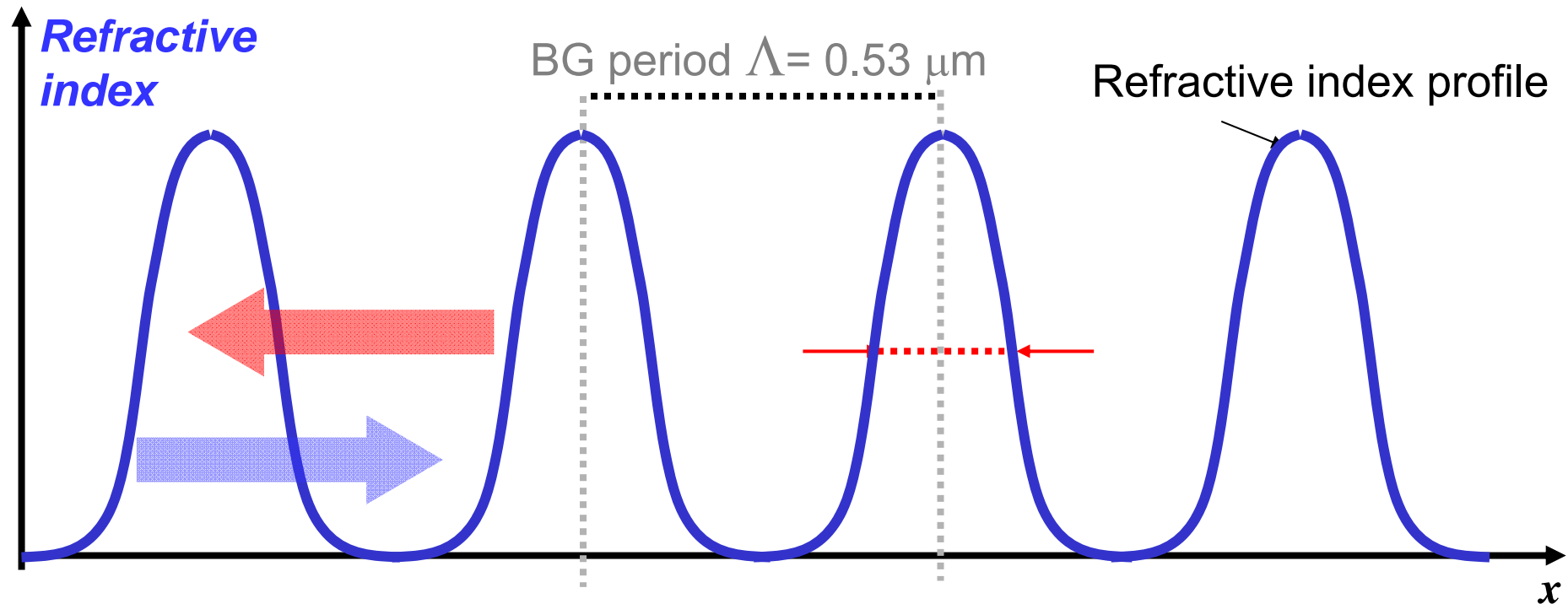
Numeric

Outline

- ❑ Why femtosecond laser microprocessing?
- ❑ Modelling of femtosecond microfabrication
- ❑ Fiber-based photonic devices
 - Fibre Bragg Gratings
 - Long-Period Gratings
 - Short cavity Er:Yt fibre laser
- ❑ Planar structures
 - Waveguide fabrication
 - Sub-wavelength gratings
 - Experiments with high repetition rate system
- ❑ fs-assisted postprocessing (microfluidic applications)
- ❑ Future work

Photonic constraints.

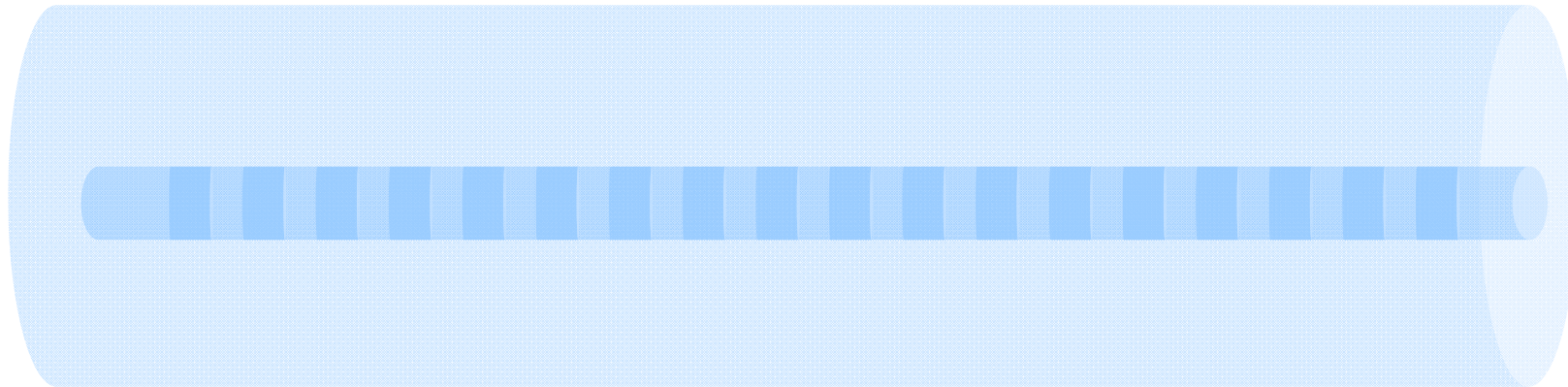
Bragg Grating as an example



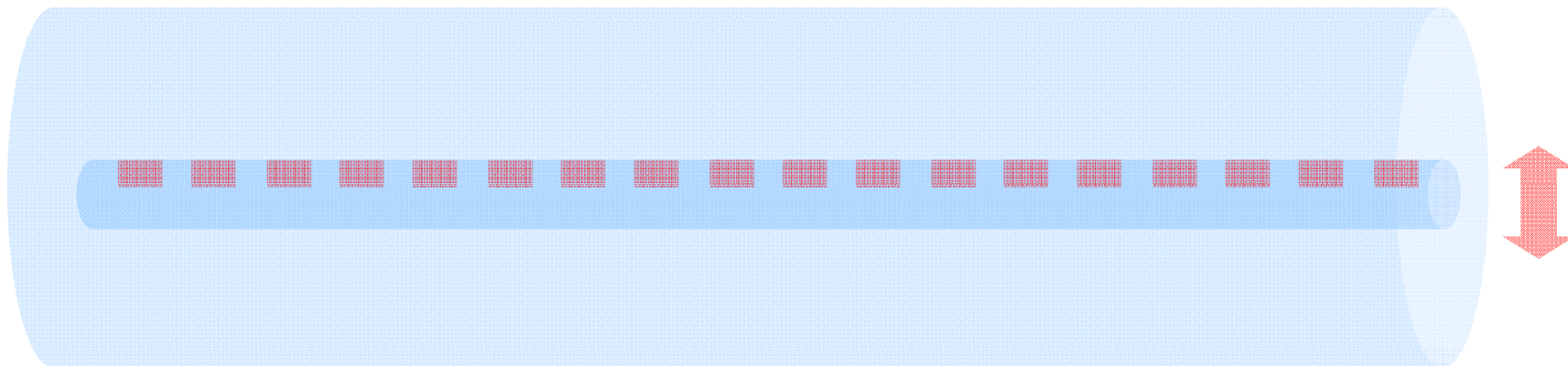
Requirement to operate at 1550 nm leads to grating period of 530 nm. It implies a refractive index pitch size of **<250 nm**

Conventional vs fs-made FBGs

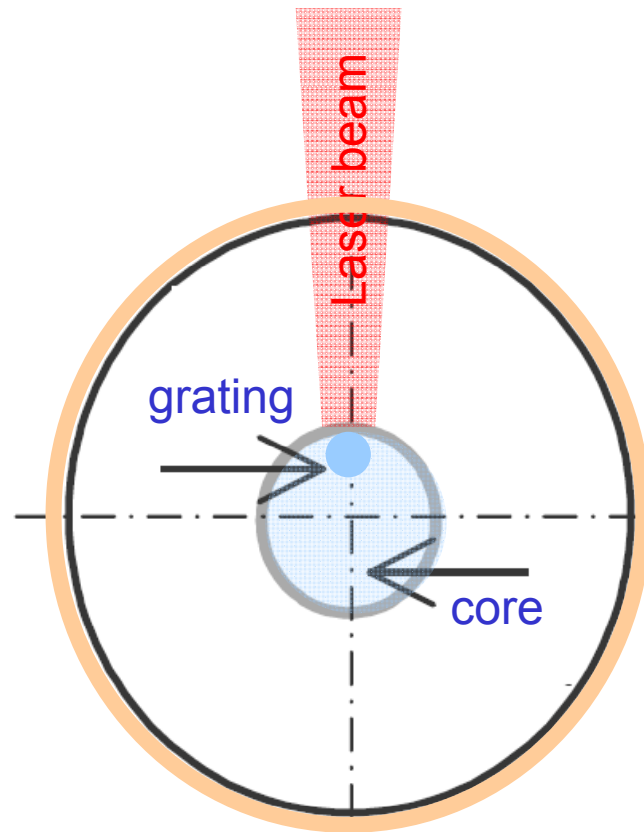
❑ Conventional FBG



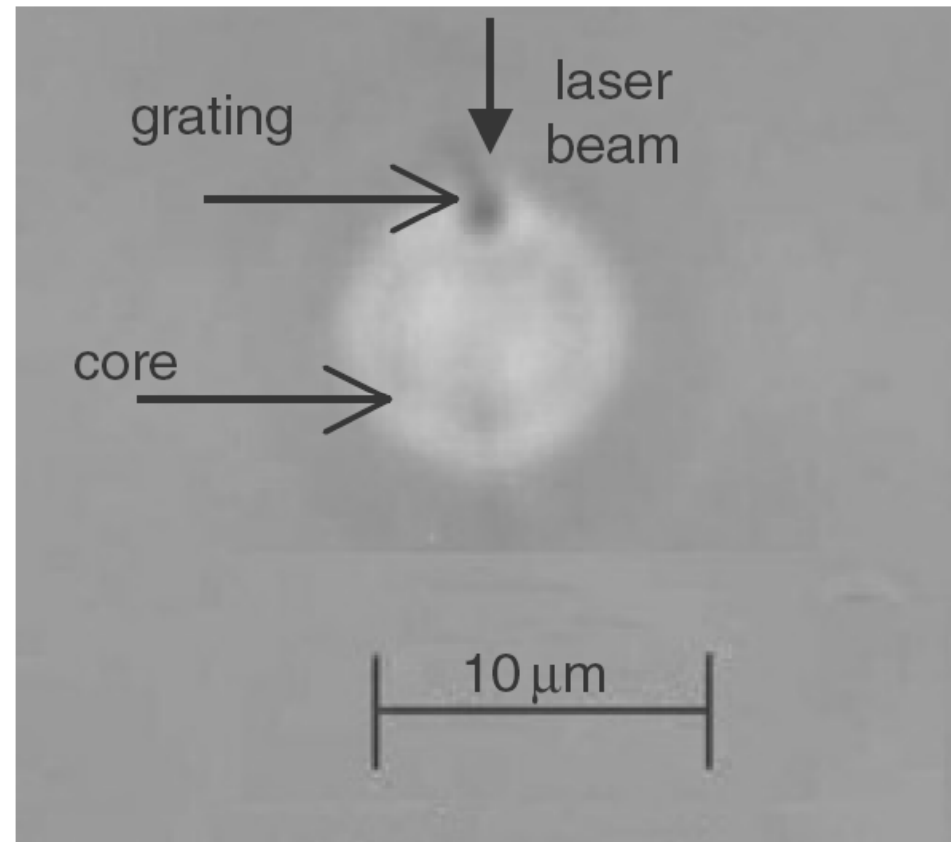
❑ Fs-made FBG



Fs-fabricated FBGs



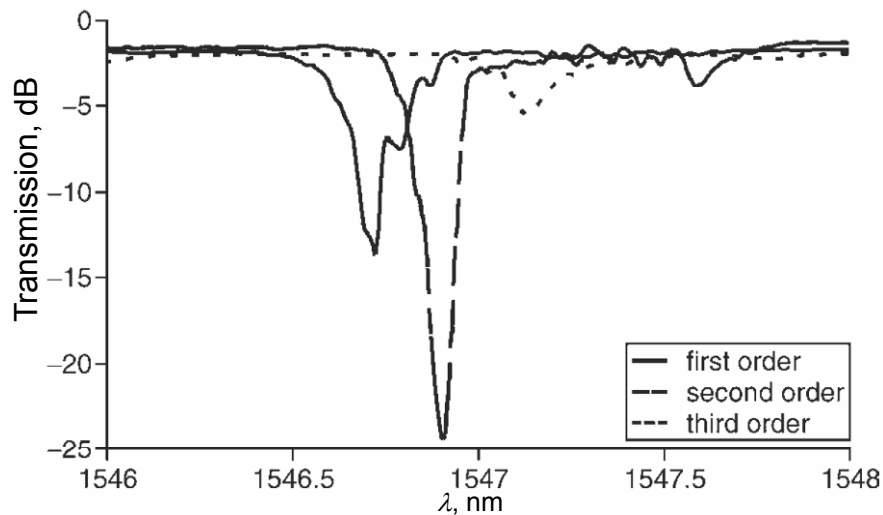
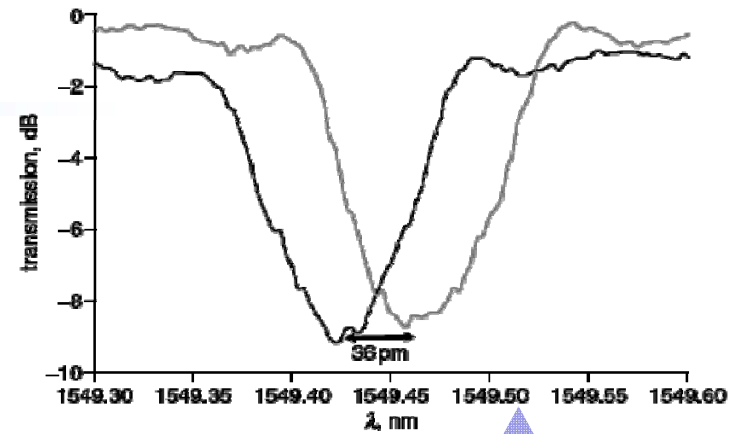
A.Martinez et al, 2005



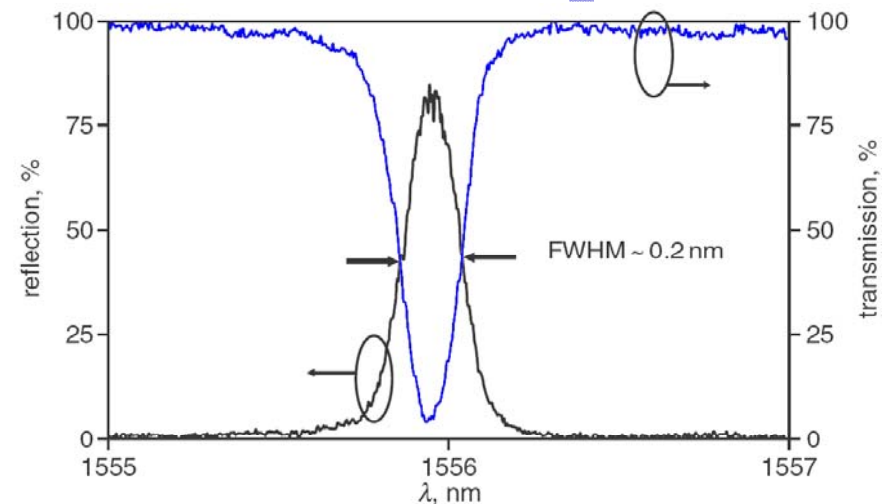
Fs-fabricated FBGs

□ Key features

- Asymmetry
- Thermal stability
- Hard to make 1st period gratings requiring submicron pitch



Transmission spectra for FBG gratings of different orders (1, 2, 3)

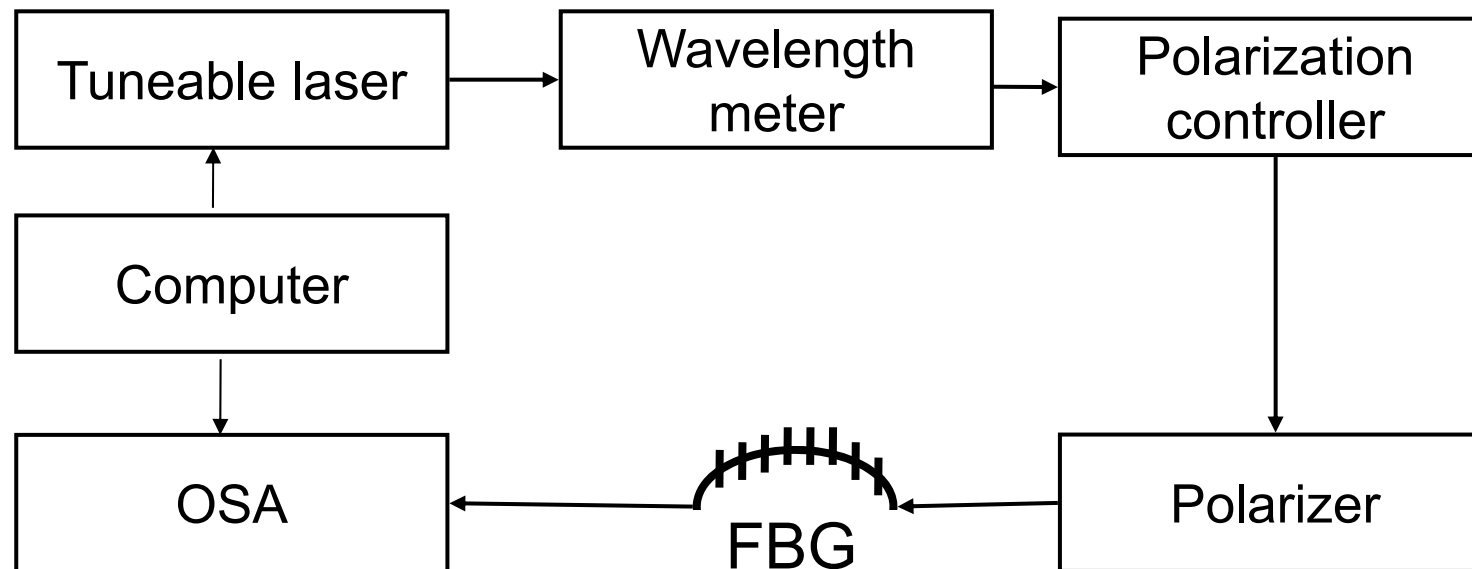


Transmission and reflection spectra for 2nd order FBG

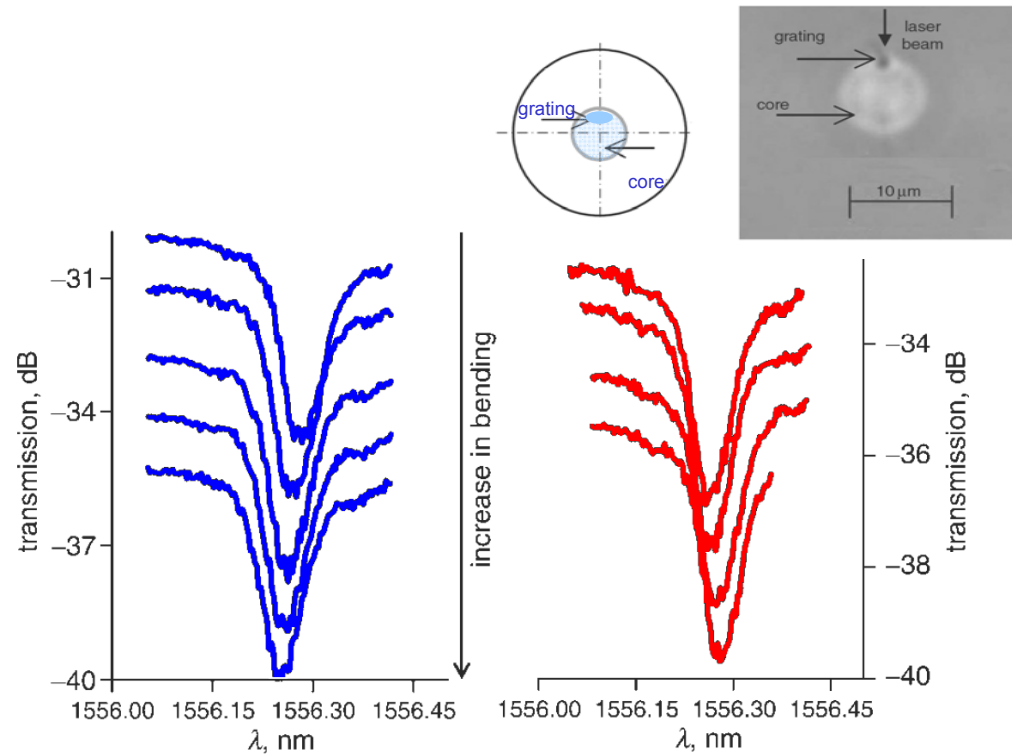
Fs-FBG based bending sensor



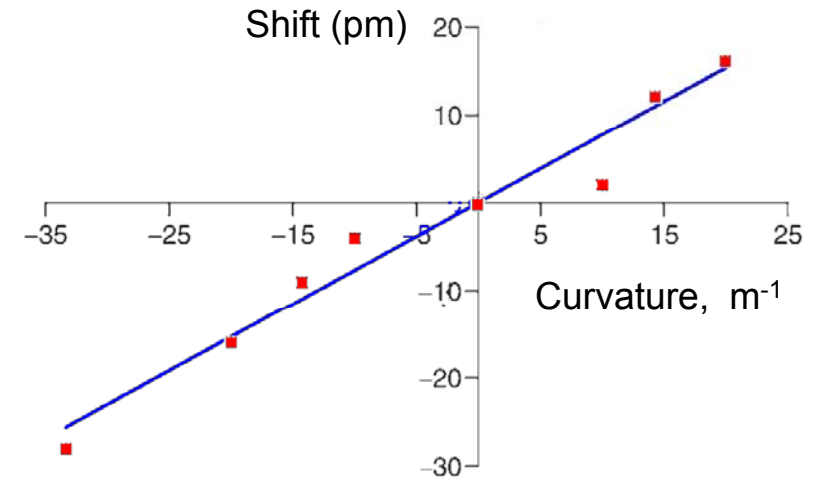
Grating asymmetry and birefringence suggest sensitivity to directional bending



Fs-FBG: Directional bend sensitivity

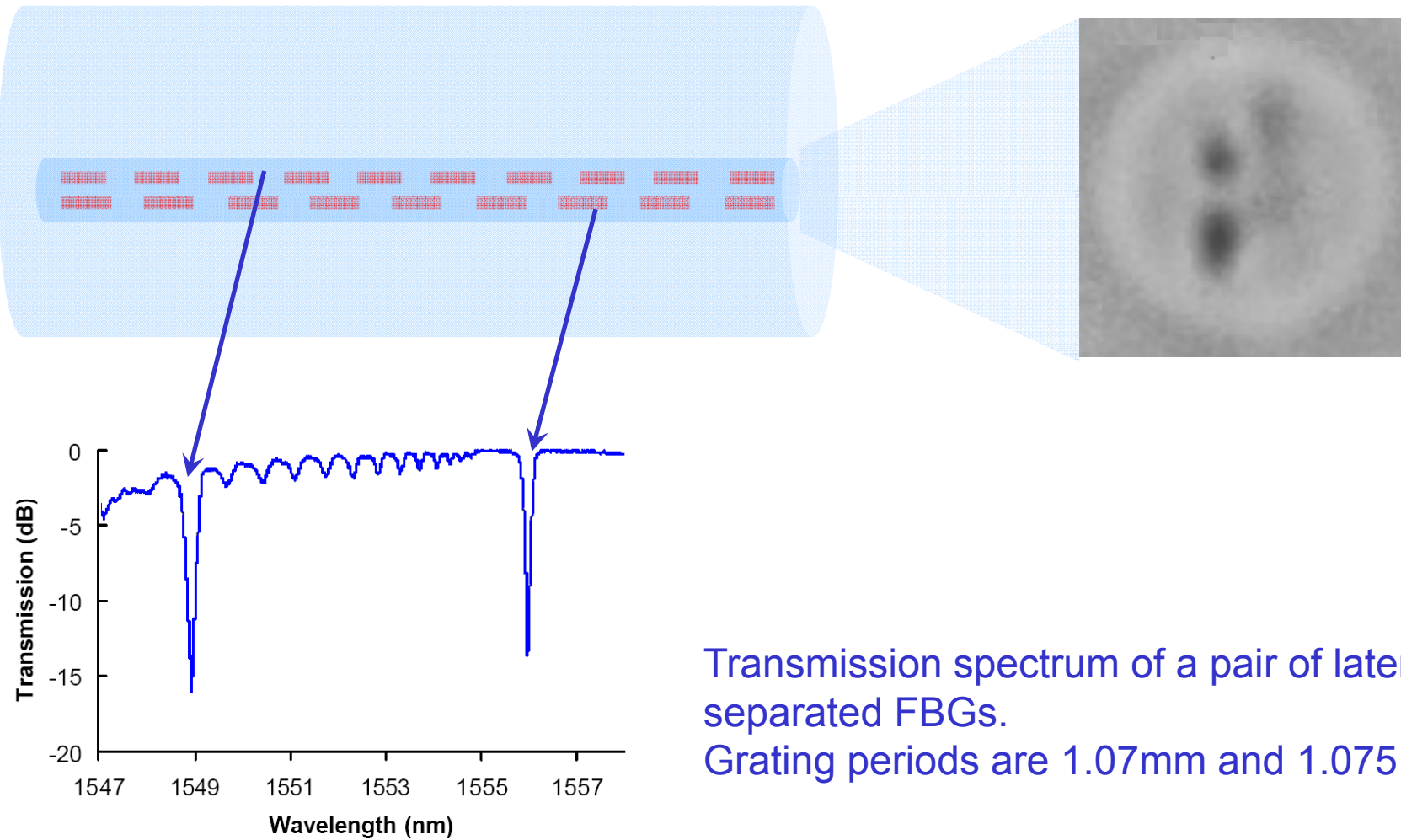


Blue and red Bragg wavelength shifts depending on bending direction



Wavelength shift against bending strength and direction.

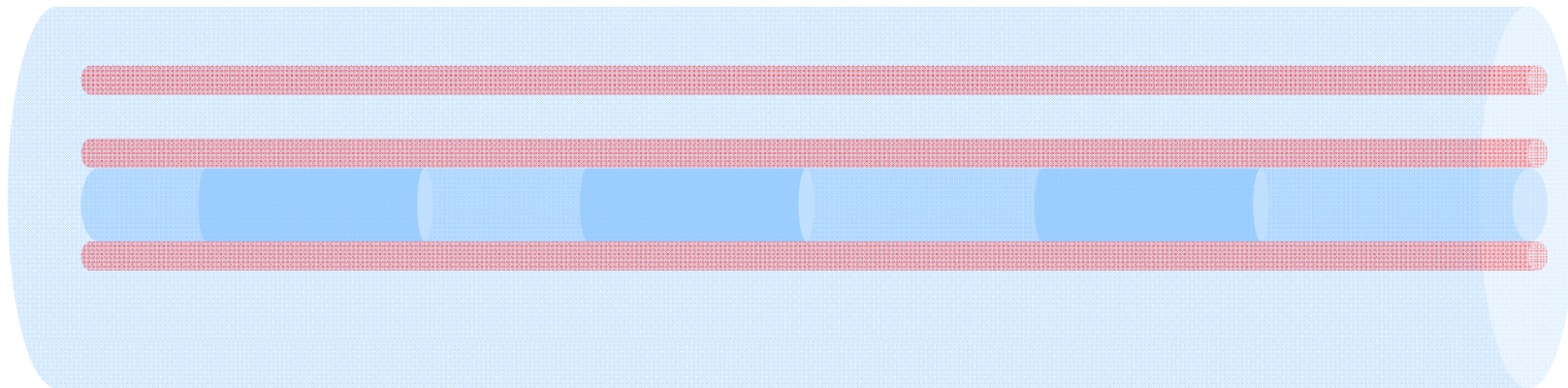
Superimposed FBGs



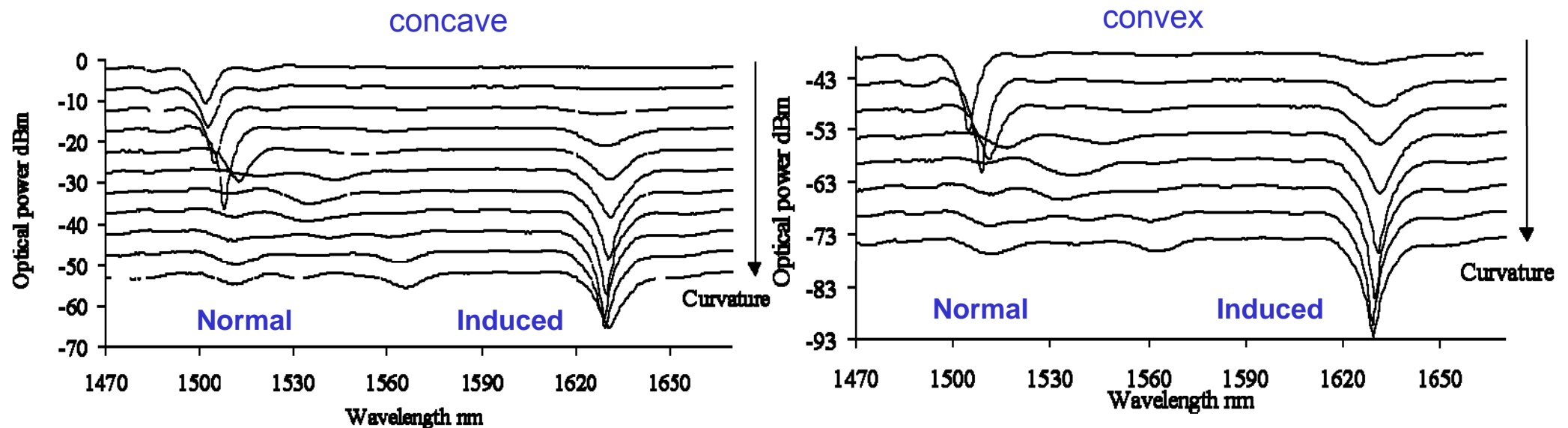
Transmission spectrum of a pair of laterally separated FBGs.
Grating periods are 1.07mm and 1.075 mm.

Fs-modified LPG as a directional bending sensor

- ❑ Long-period grating (LPG) fabricated using conventional UV inscription was modified with fs-fabricated rods/grooves in cladding



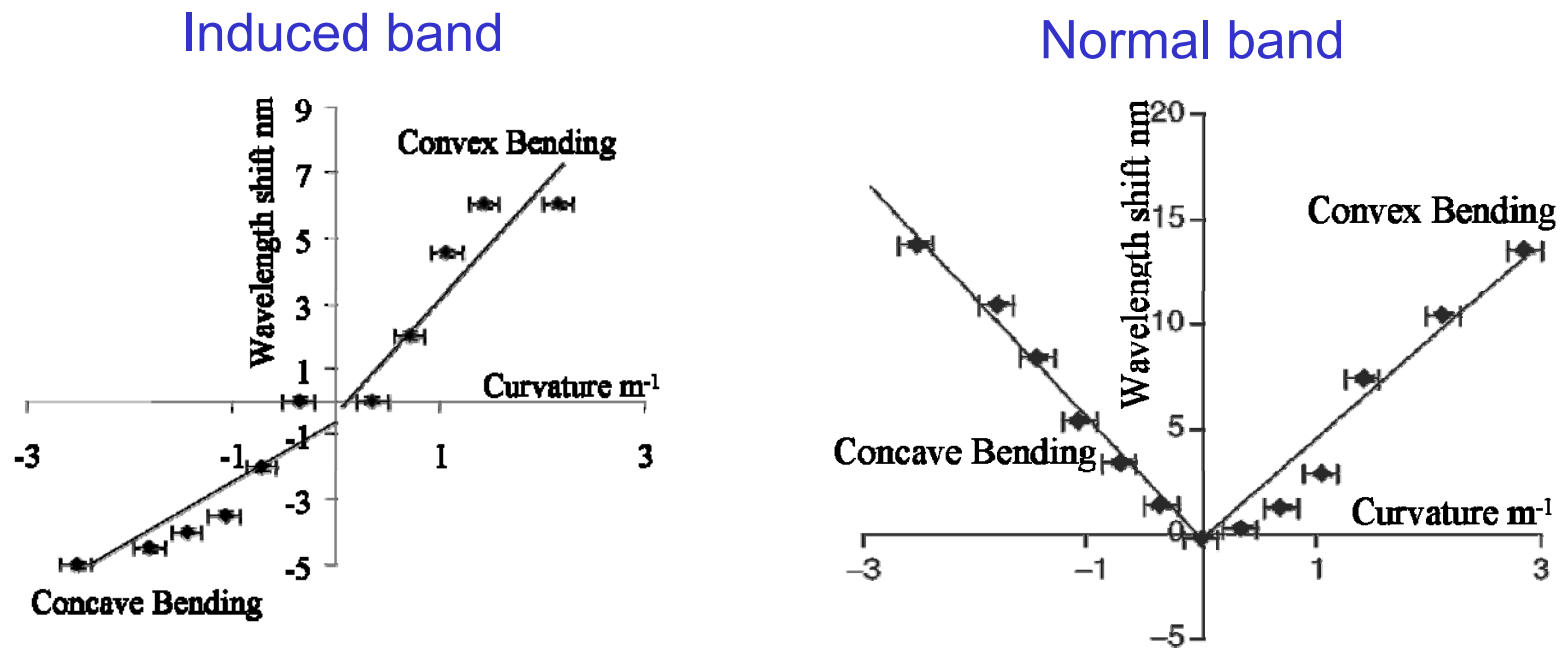
Fs-modified LPG Transmission spectra



Transmission spectrum of LPG fibre device against direction and amount of curvature

Fs-modified LPG

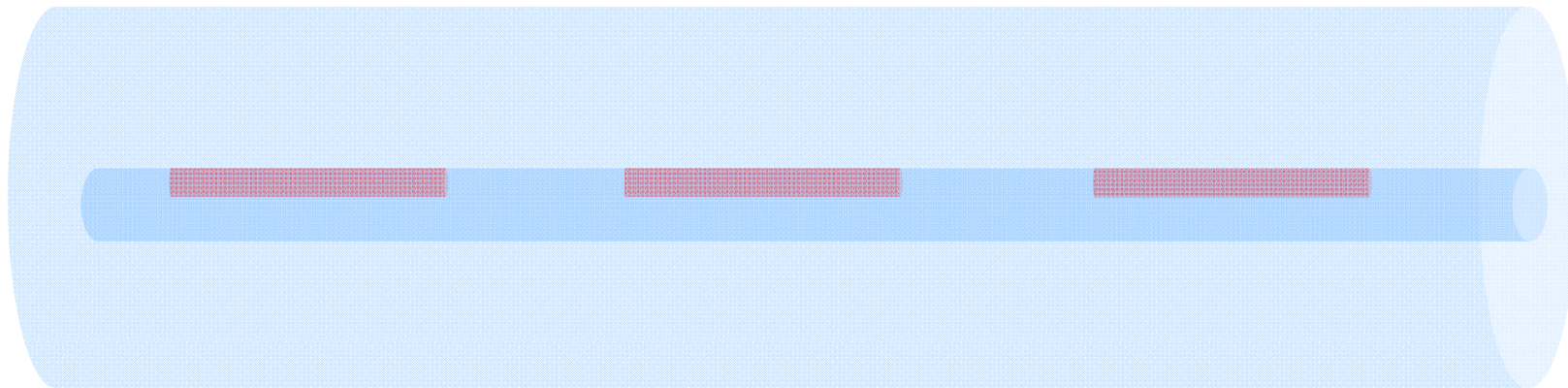
Directional bending sensitivity



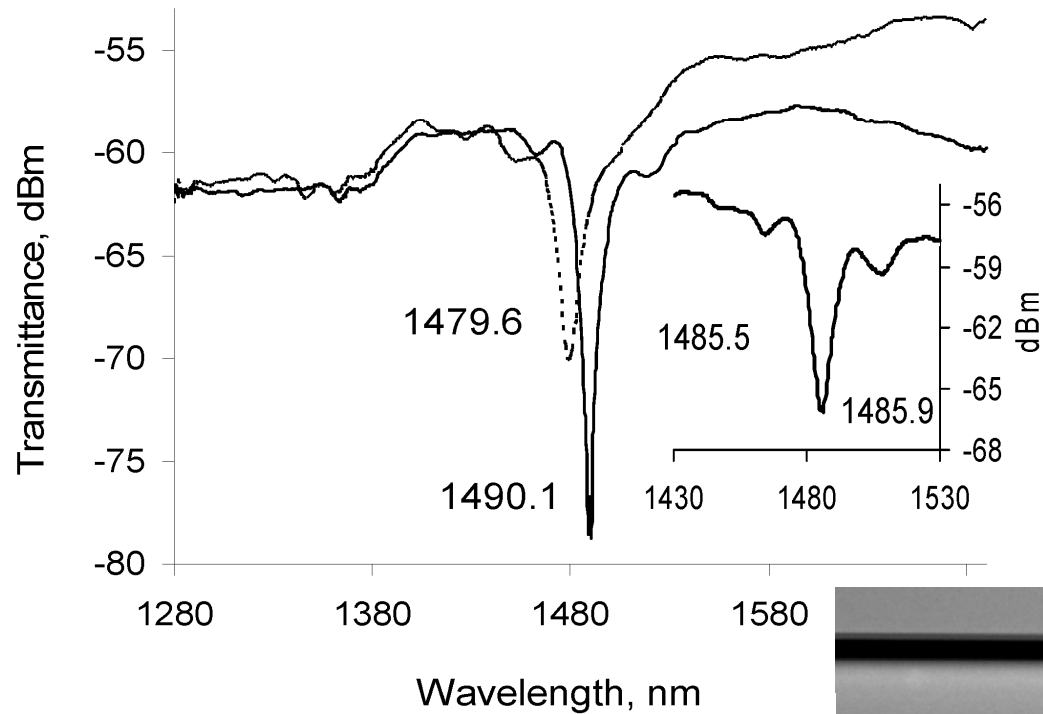
Spectral sensitivity (wavelength shift) of induced attenuation bands (left) and normal attenuation band (right) at 1500 nm

All-fs fabricated LPG

- “Cylindrical grooves” inscribed at the core-cladding interface form a nearly perfect LPG with distinct polarization features

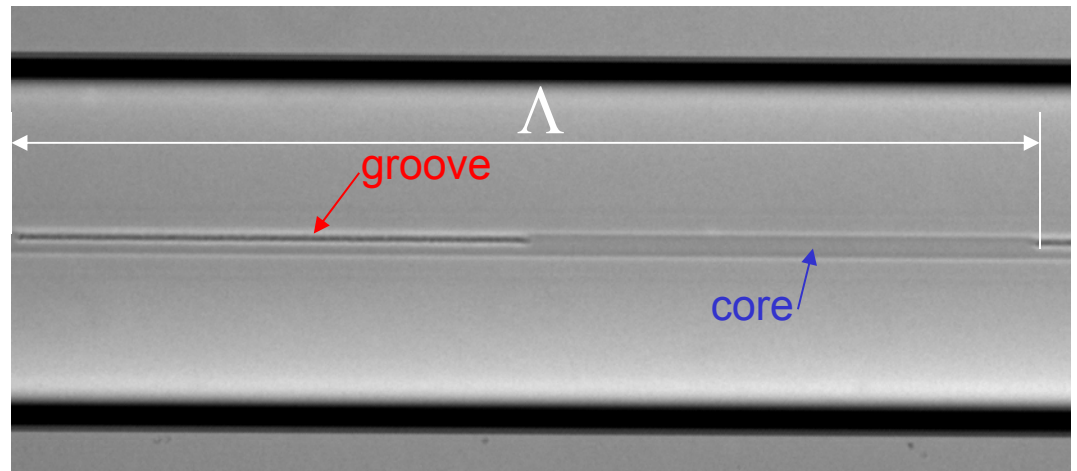


All-fs fabricated LPG



The transmission spectrum of the fs-made LPG. The insert shows the spectrum of the standard UV-inscribed LPG.

Microscopic image of the fibre with LPG. The grooves are offset with respect to the core axis.



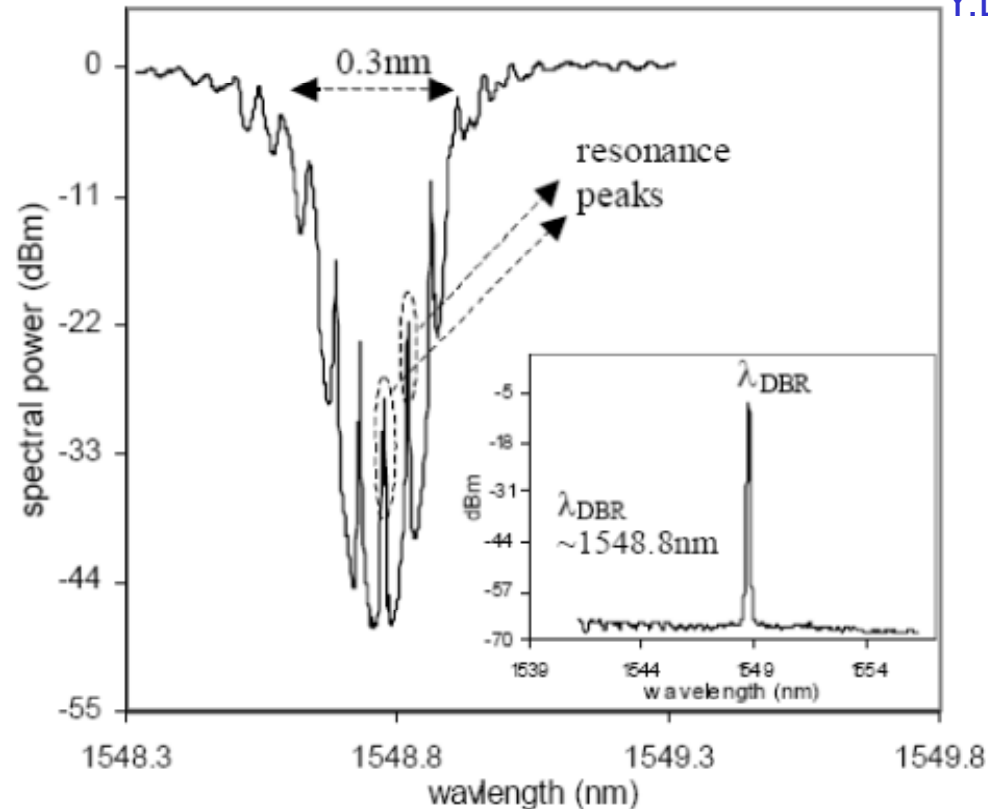
Heavy duty Er:Yb fibre laser



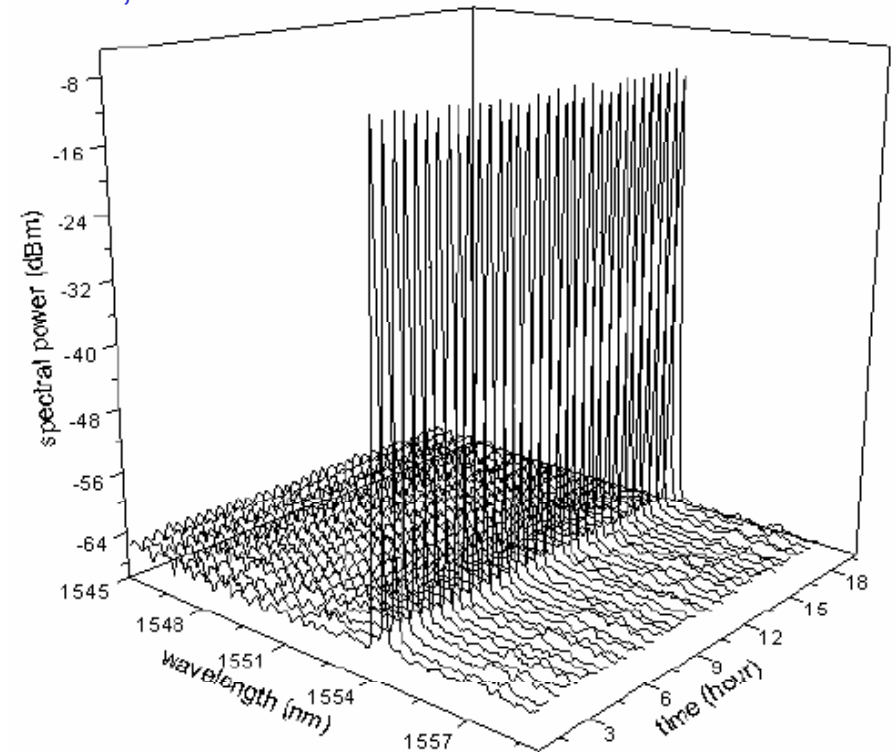
Two 8mm-long uniform FBGs spaced 15mm apart was realized in a one-step, 30 second inscription process into the Er:Yb-codoped fibre to create a DBR fibre laser configuration.

Fs-made fibre laser

Y.Lai et al, BGPP-2005



Transmission profile of the DBR fibre laser cavity showing distinct resonance peaks. Inset shows the fibre laser output optical spectrum during operation.



The fibre laser output sampled every half hour over 17 hours at $\sim 500^\circ\text{C}$

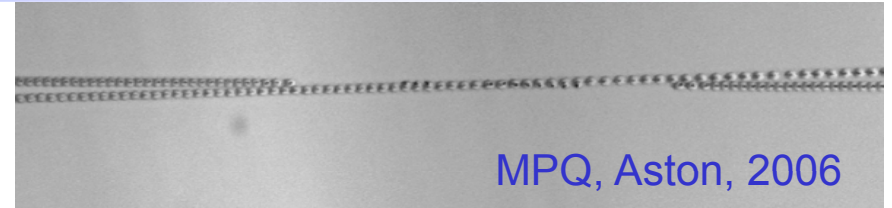
Outline

- ❑ Why femtosecond laser microprocessing?
- ❑ Modelling of femtosecond microfabrication
- ❑ Fiber-based photonic devices
 - Fibre Bragg Gratings
 - Long-Period Gratings
 - Short cavity Er:Yt fibre laser
- ❑ Planar structures
 - Waveguide fabrication
 - Sub-wavelength gratings
 - Experiments with high repetition rate system
- ❑ fs-assisted postprocessing (microfluidic applications)
- ❑ Future work

Photonic structures in planar geometry

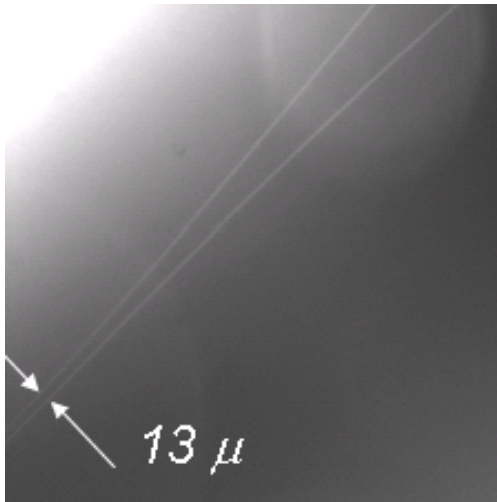


Waveguides
and structures



Chain of pearls

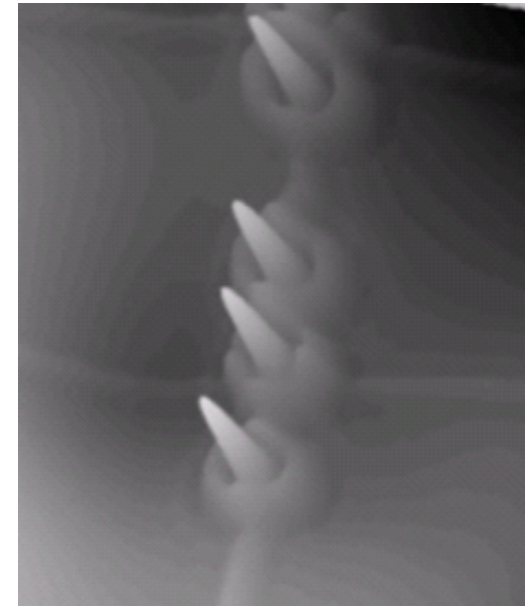
Bragg grating



Waveguides and couplers



260 nm pitch size grating (first order Bragg grating) in planar fused silica

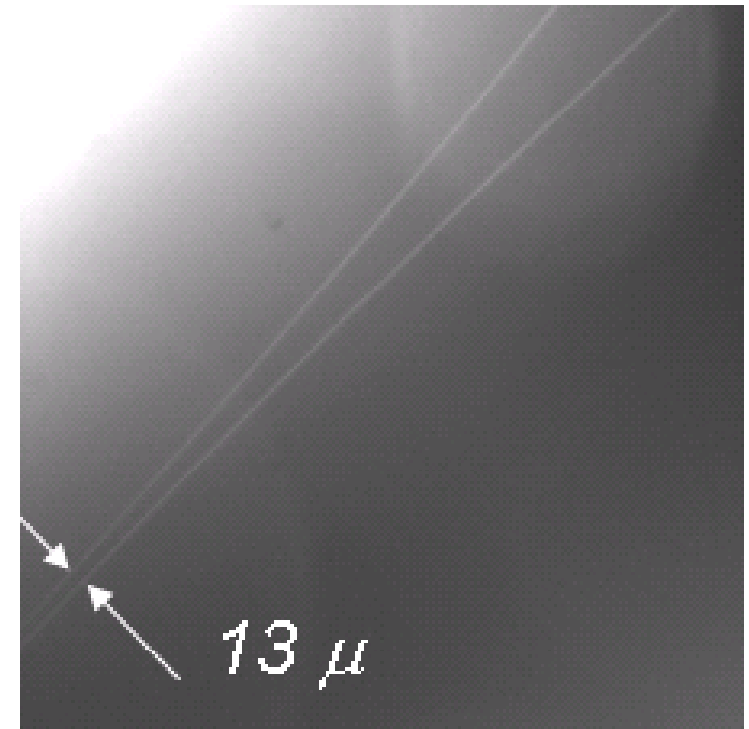


Ref. index map of the pearls

OAD filter as BG assisted coupler



A design prototype of Optical Add/Drop filter in the form of grating assisted coupler.

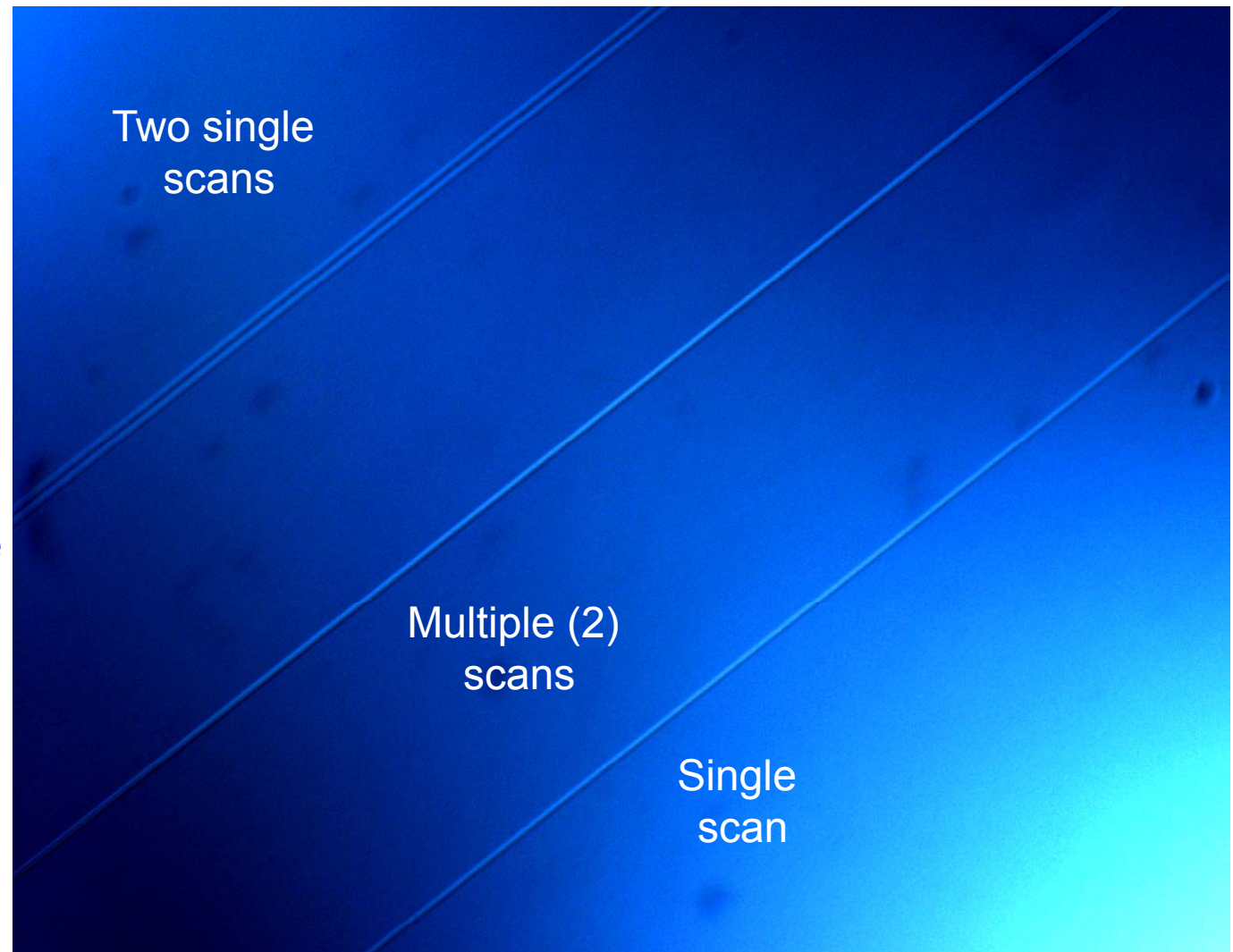


Examples of waveguides

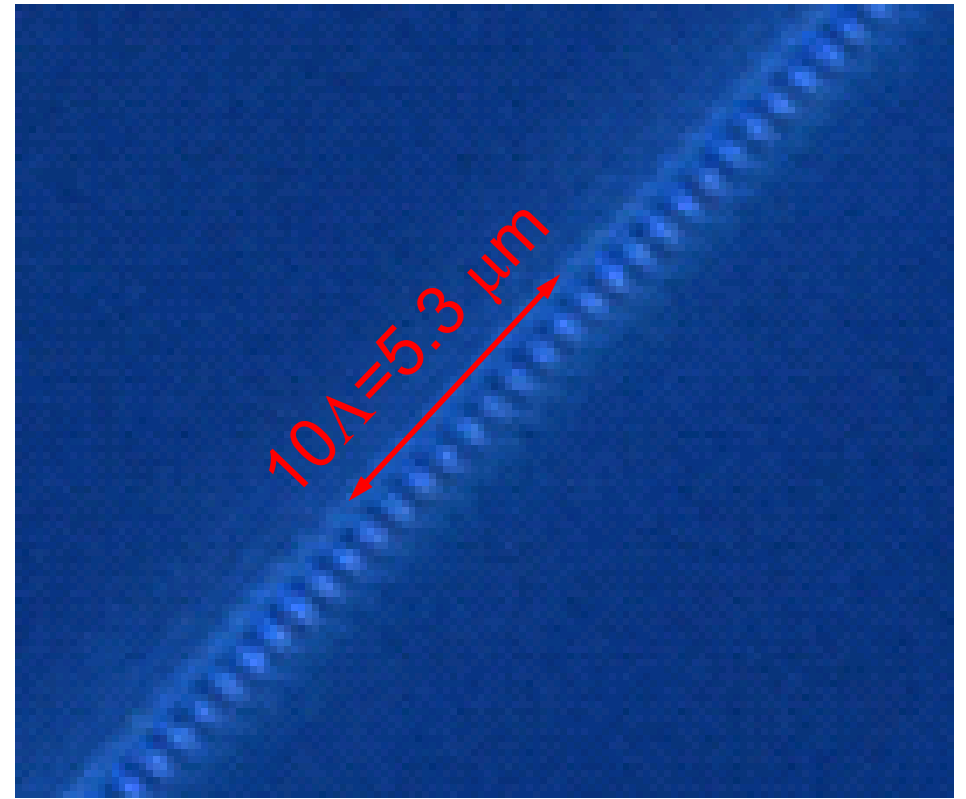
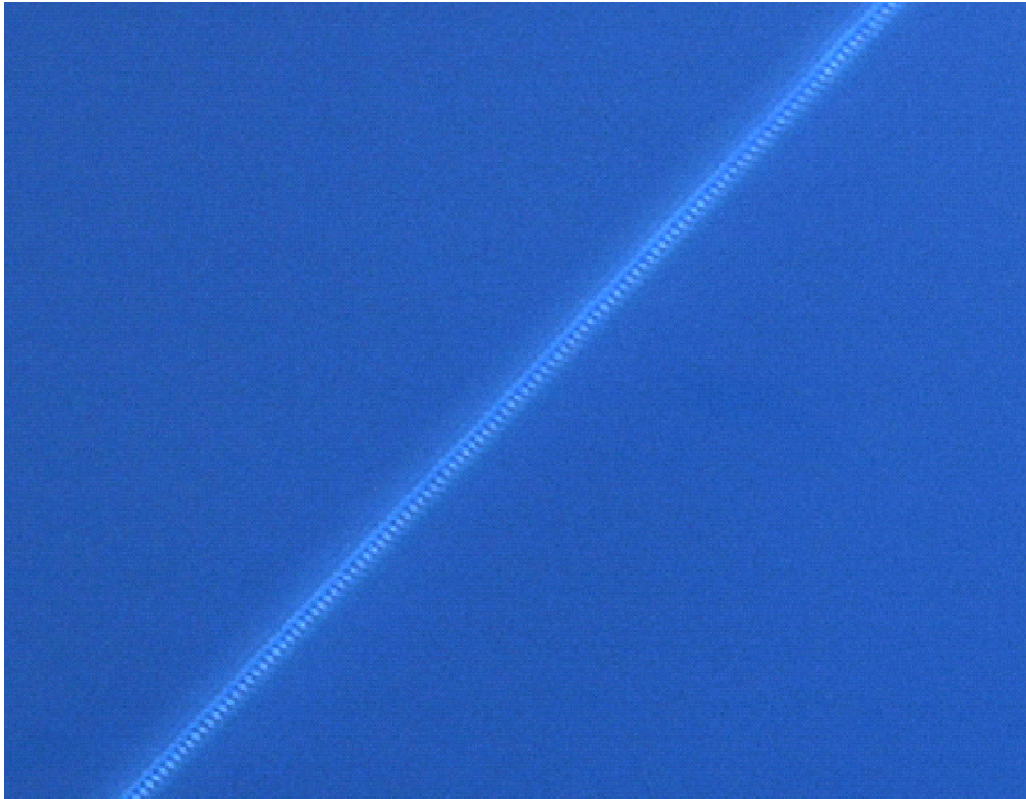
LRR, NA~0.08

Low contrast is a major limiting factor in making good waveguides and photonic devices in general

Multiple scans is one way of increasing of inscribed refractive index

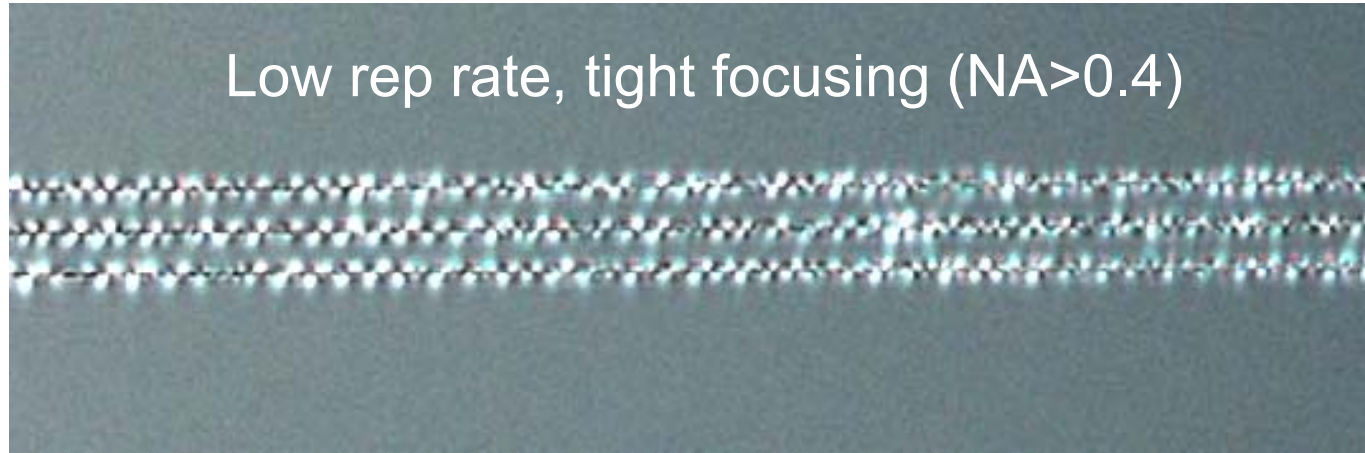


First order Bragg Grating



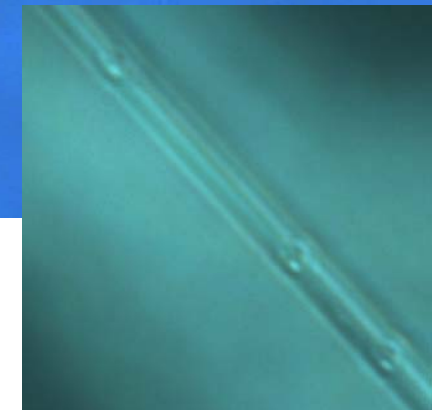
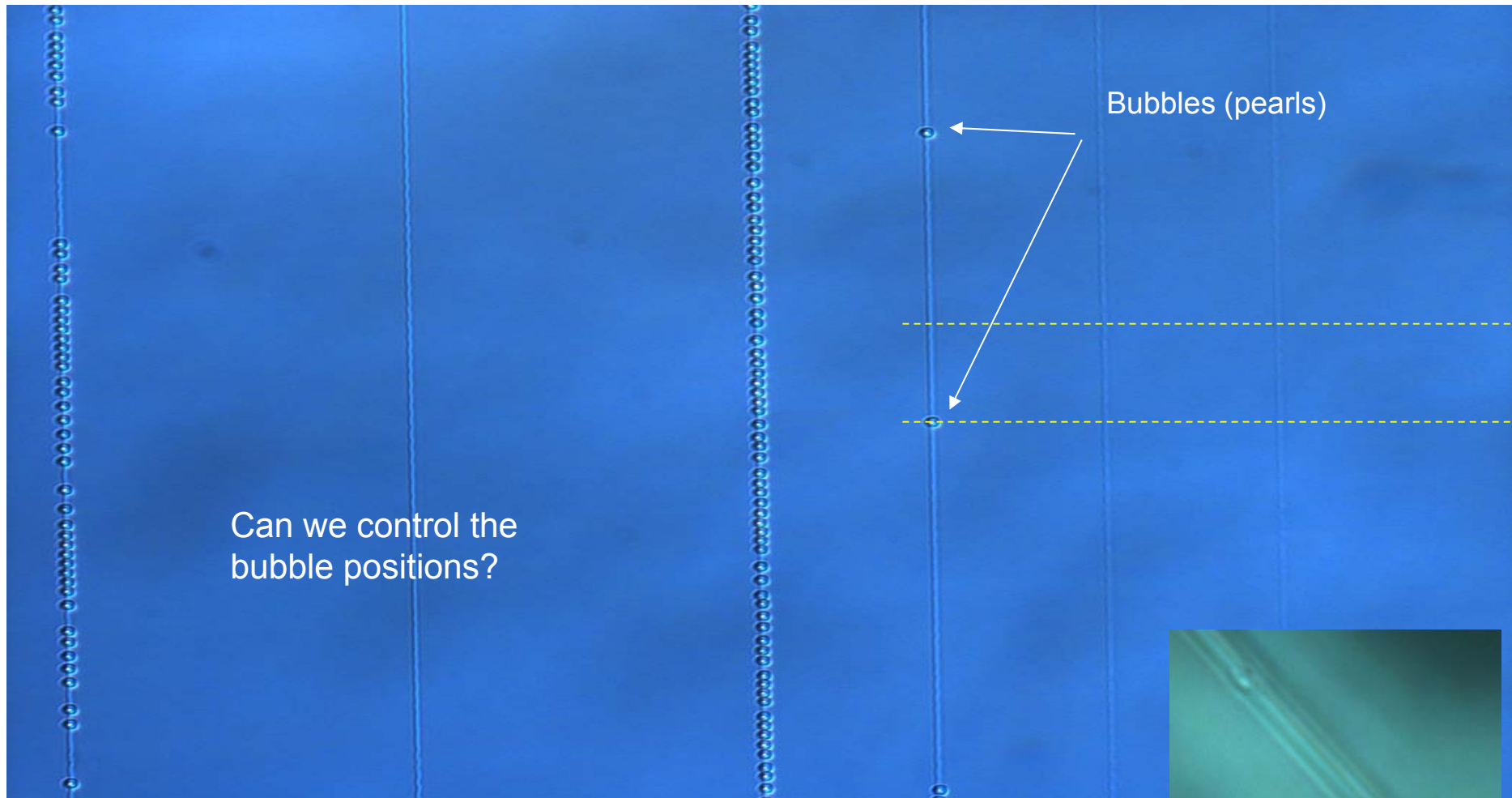
1st order BG is produced by means of point-by-point **800nm** fs inscription.
Refractive index variation is estimated to be 5×10^{-4} which makes it feasible for photonic applications

Show stoppers

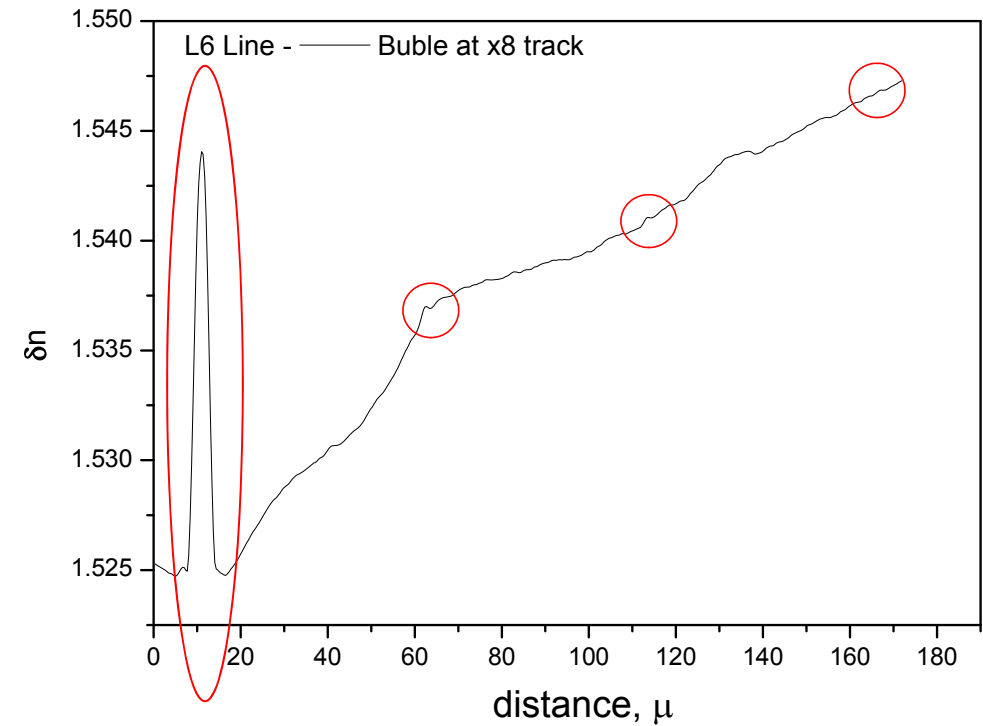
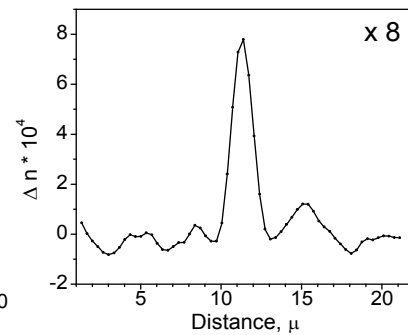
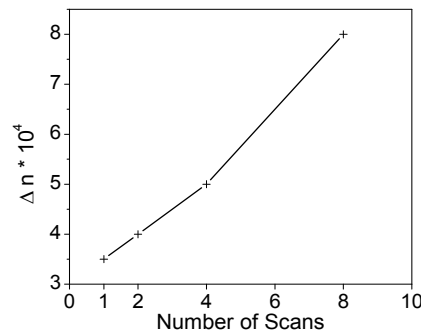
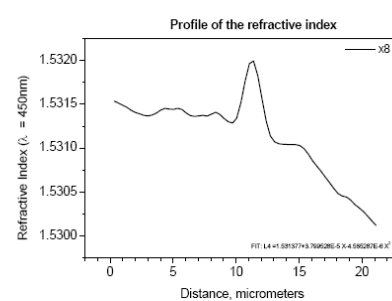
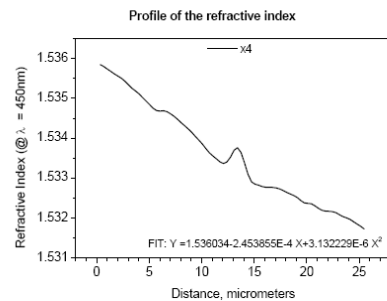
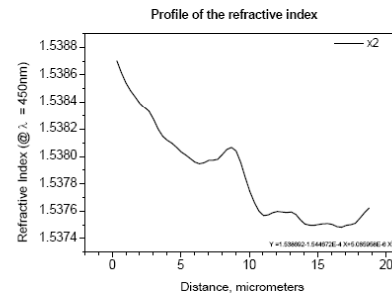
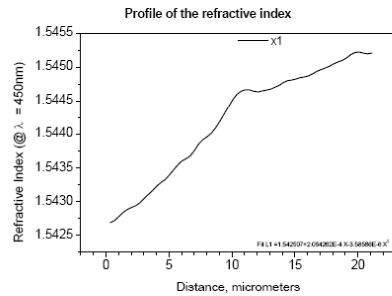


- ❑ Residual stress seems to be a major problem for waveguides fabricated with low frequency (1 kHz repetition rate) laser systems.
- ❑ Fused silica appears to be very awkward material due to its feature to lock stresses
- ❑ MHz rep. rate fs laser system and doped glasses or polymers may be a solution to eradicate residual stresses

Variation of the Refractive Index. Multiscans and pearls



Refractive index variations, multiple scans (HRR)

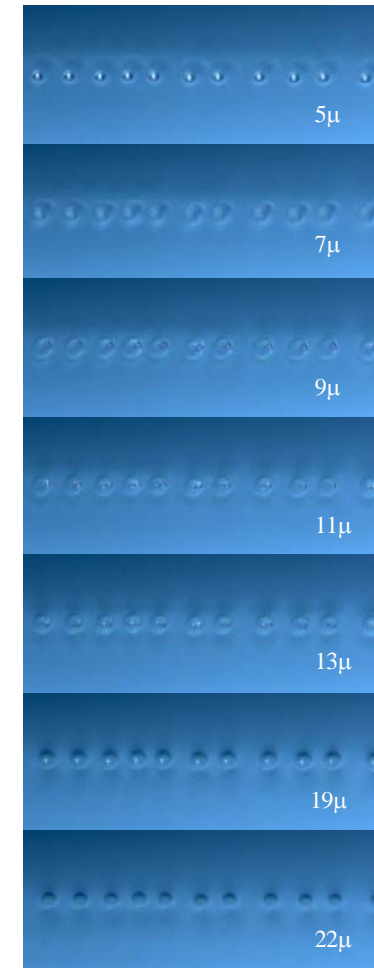
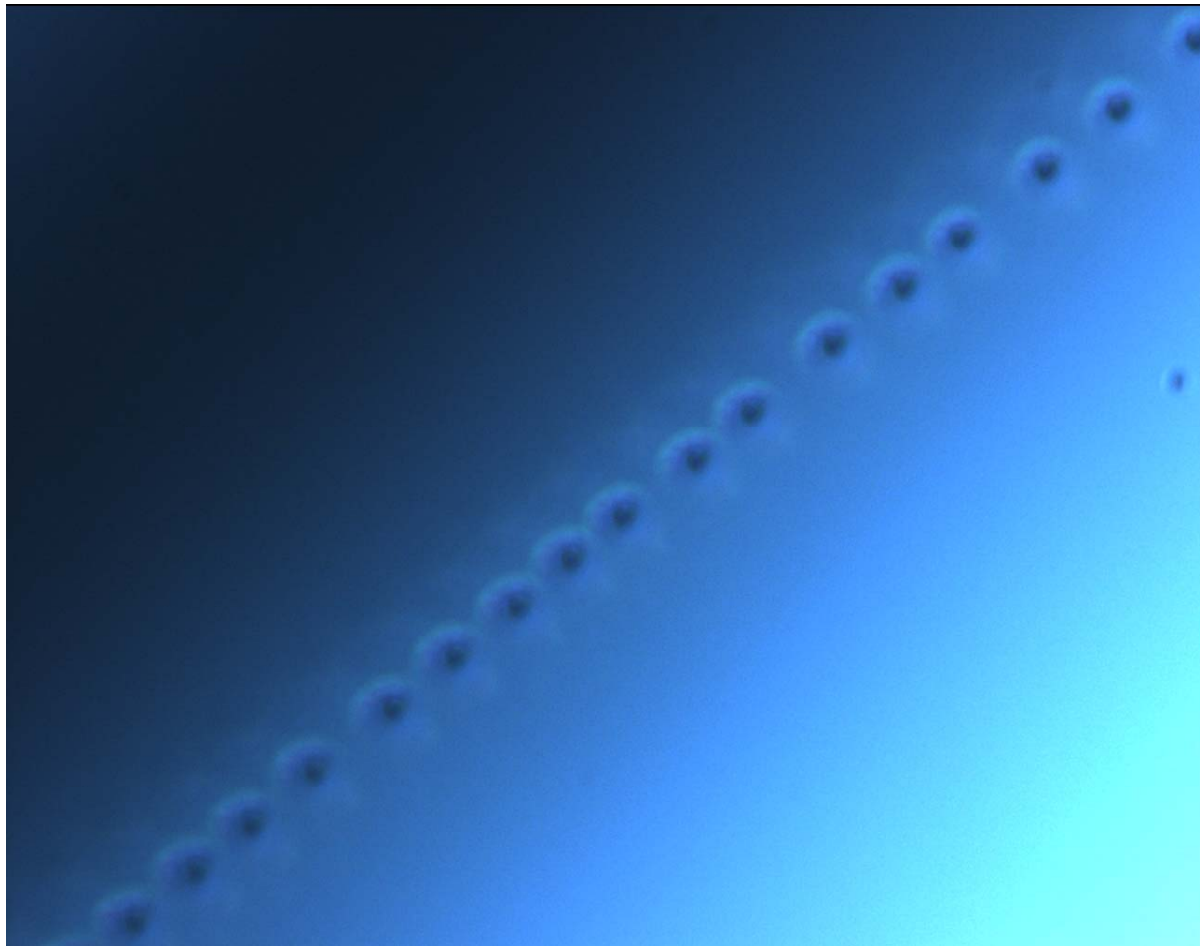


Pearls - nice objects, but...

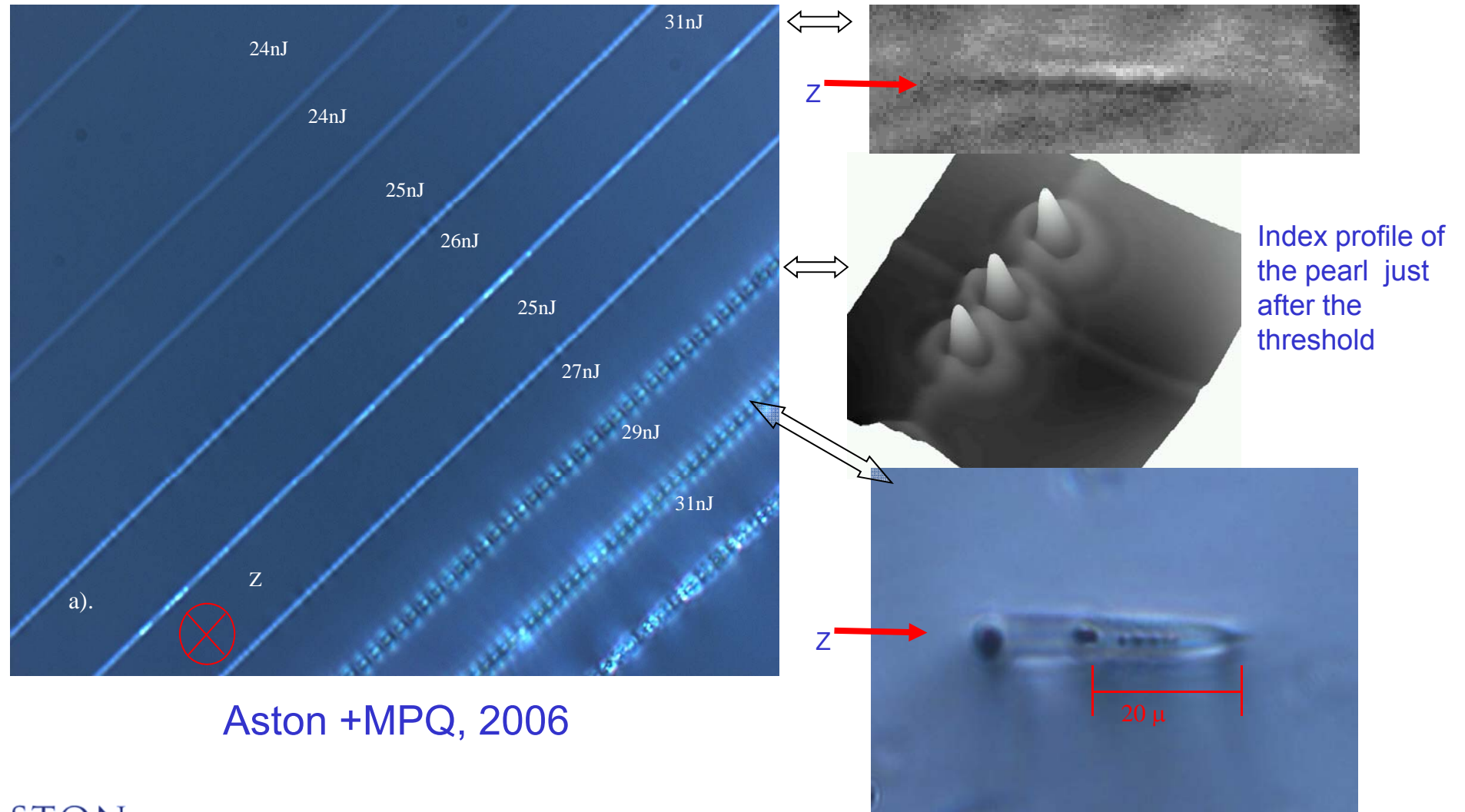
Main questions are:

- Can we control their position?
- Pearl's structure? (if any).
- Can we couple and propagate light in a chain of pearls?
- What is the mechanism of pearls formation?

Microscopic images shot at different depths

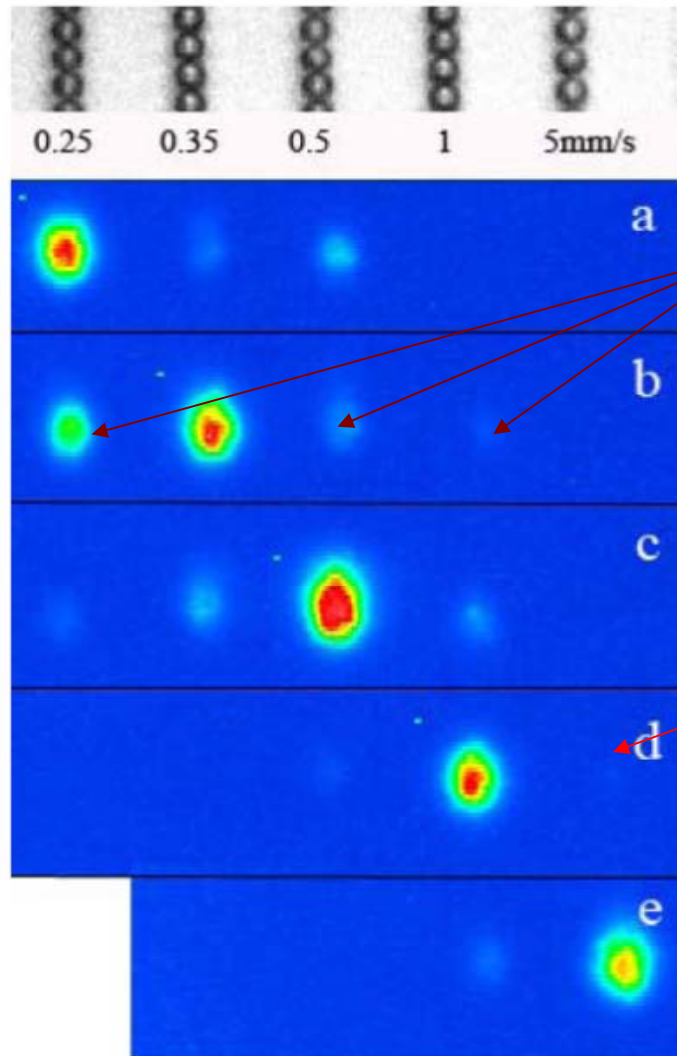


Pearl chain formation



Aston +MPQ, 2006

Pearl-chain waveguides



R. Graf, A. Fernandez, M. Dubov, H. J. Brueckner, A. Apolonski, B.N. Chichkov

**) Max-Planck-Institute of Quantum Optics, Hans-Kopfermann-Str. 1, D-85748 Garching, Germany*

Photonics Research Group, Aston University Birmingham B4 7ET, UK

Fachhochschule Oldenburg/Ostfriesland/Wilhelmshaven, University of Applied Sciences, Constantiaplatz 4, D-26723 Emden, Germany

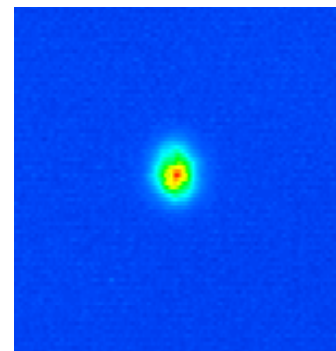
Laser Zentrum Hannover e.V., Hollerithallee 8, 30419 Hannover, Germany

Ludwig-Maximilians-Universität München, D-85748 Garching, Germany and

Appl. Phys, 2007

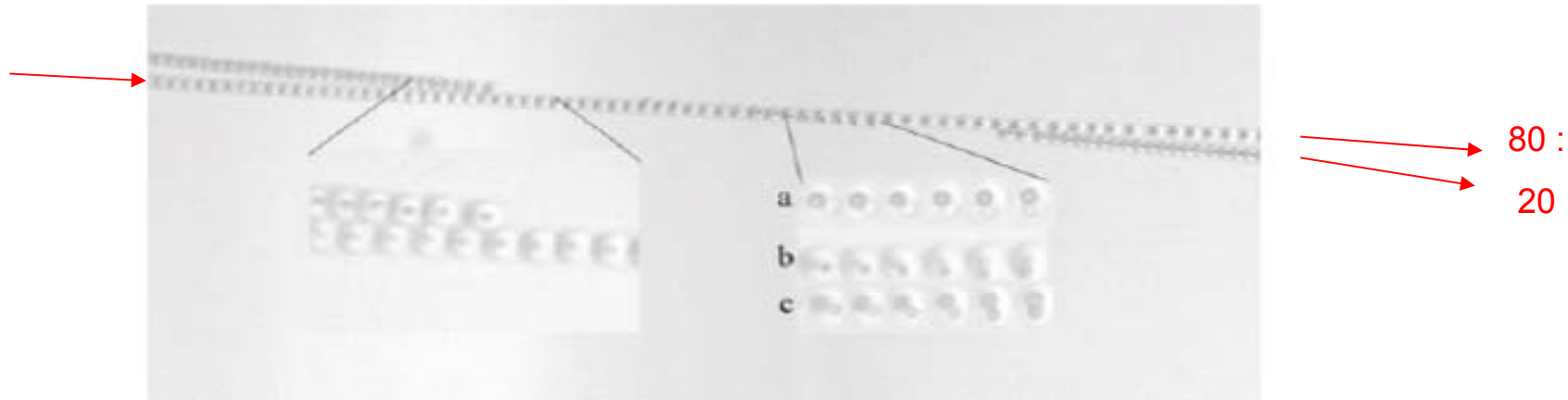
Cross-talk
between
waveguides
separated
by 18μ gaps

7 dB/cm – the best so far

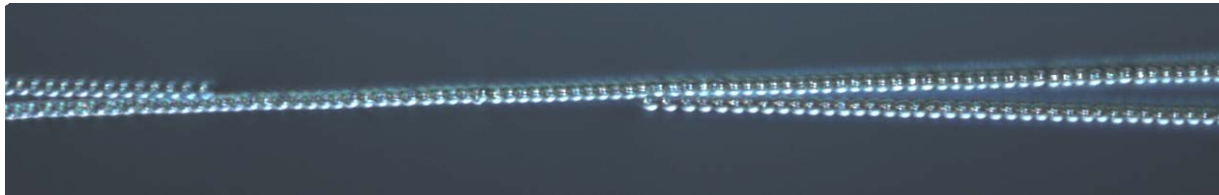


MFD = 12μ
index contrast as a
result of simulations
 $n_{\text{eff}} = + 0.02$

X-Coupler



First coupler was demonstrated with 80:20 coupling ratio at 1559nm without any optimisation.

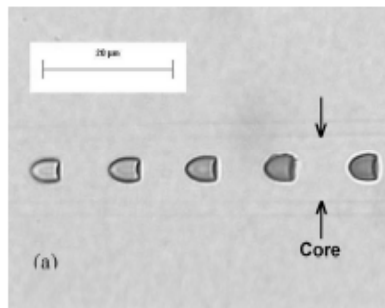


Periodic structures formation

All known self-assembled structures are being formed in *longitudinal* direction

ОПТИЧЕСКИЙ РАЗРЯД В ВОЛОКОННЫХ СВЕТОВОДАХ

И.А. БУФЕТОВ, Е.М. ДИАНОВ,
Научный центр волоконной оптики им. А.М. Прохорова РАН



Why do we need them?

Periodic Nanovoid Structures via Femtosecond Laser Irradiation

Shingo Kanehira,^{*,†} Jinhai Si,[‡] Jianrong Qiu,[§] Koji Fujita,[†] and Kazuyuki Hirao[†]

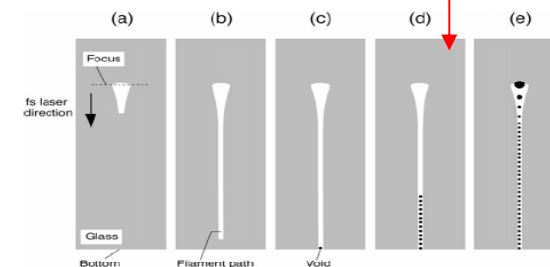
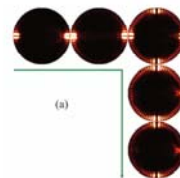
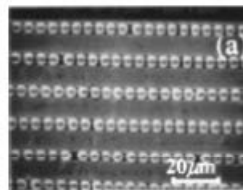


Figure 4. Schematic illustrations for the formation process of the periodic void structure. Void formation proceeds from Figure 4a—e.



Highly efficient optical coupling and transport phenomena in chains of dielectric microspheres

February 1, 2006 / Vol. 31, No. 3 / OPTICS LETTERS



Optical coupling and transport phenomena in chains of spherical dielectric microresonators with size disorder

APPLIED PHYSICS LETTERS

VOLUME 85, NUMBER 23

6 DECEMBER 2004

Experiments

This is a multiple-pulse process

Threshold: $1.7\text{MW} < P_{\text{cr}}$;

but no data on $P_{\text{cr}}(T)$

White light generation,

threshold for white light and bubbles is the same

more white light at higher speed,

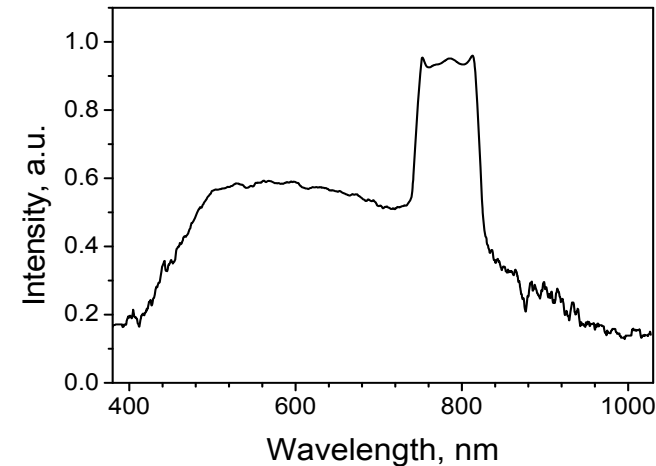
self-limiting process at lower speed;

Pearl structure along the laser beam

self-limiting process of the pearl formation;

“frozen” shock wave in lower part, almost spherical around top (biggest void);

Pearls separation – self “assembly” features



$$\lambda_{\text{max}} = \frac{hc}{kxT} = \frac{2.89776829 \dots \times 10^6 \text{ nm} \cdot \text{K}}{T}$$

$T_{\text{fit}} \sim 5000\text{K}$

Mechanism

At lower energies, laser pulses

melt the glass, producing a molten cylindrical volume, along the Z -writing direction, which then becomes more dense during the solidification process.

Possible explanation of the bubble “instability” at higher energies:

threshold-like *single-photon* absorption which occurs in glass at $T > 1500K$ ($\alpha \sim 10^4 \text{cm}^{-1}$). The fraction of absorbed energy rapidly increases, and a hot spot ($T \sim 5000K$) can be formed. This hot area moves towards the laser (auto-soliton) giving rise to the structure formed along the laser beam. The SiO_2 molecules dissociate (at $T > 1500K$) and form dense plasma.

Estimation of the internal pressure ($p = nkT$) gives a level of a few GPa. Thus the conditions for a glass densification occur.

Micro-void formation:

- plasma losses energy at outer part of the bubble where a “condensation” takes place, while middle of the pearl is hot and at high pressure. Balance of material gives $R_{dens} \sim \sqrt[3]{\rho_0 / \Delta\rho} \cdot r_{void}$, which was experimentally confirmed.
- alternatively, formation of the charged layer on a liquid-plasma interface due to different e^- , i^- mobilities. Then, the effective surface tension could have a *negative* sign, thus any increase in surface area will be energetically profitable. Recall, that a surface tension drops with $T \uparrow$.

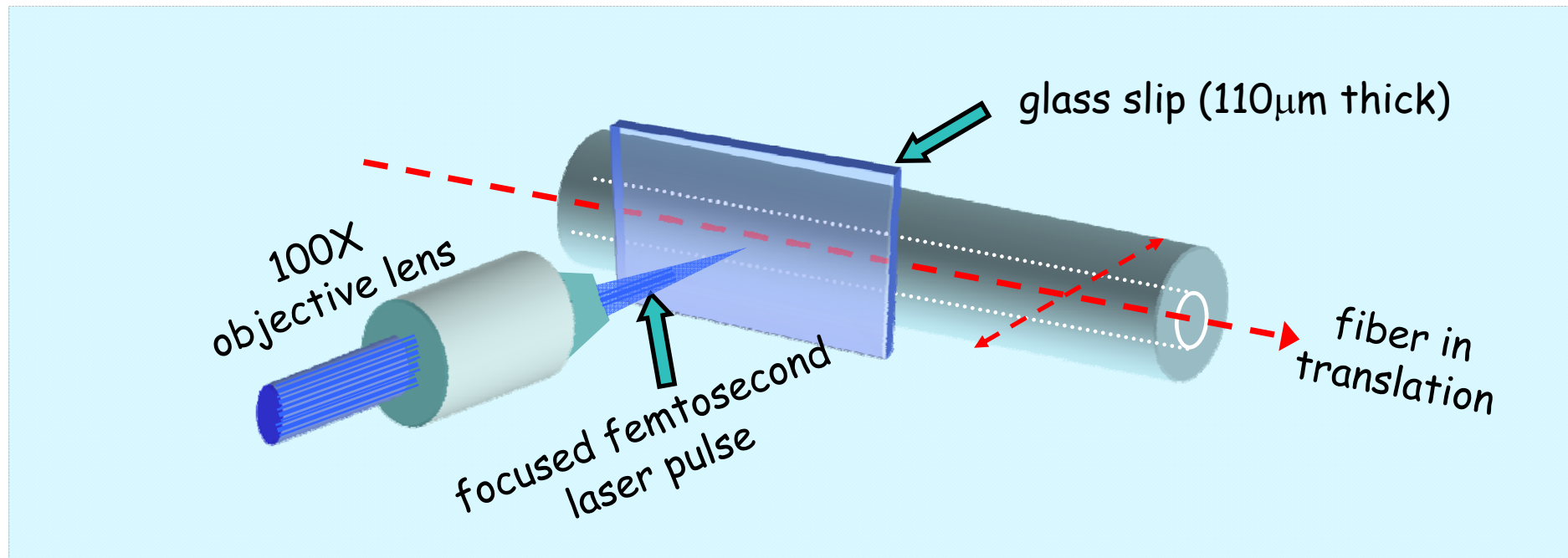
Self-stopping of the pearl growth (and white light)

is due to the void absorption is much lower and, additionally, shifted beam is being distorted. Thus beam perturbation makes new pearl appearance to be possible only at some distance from the previous one. And finally, glass can not be densified more.

Outline

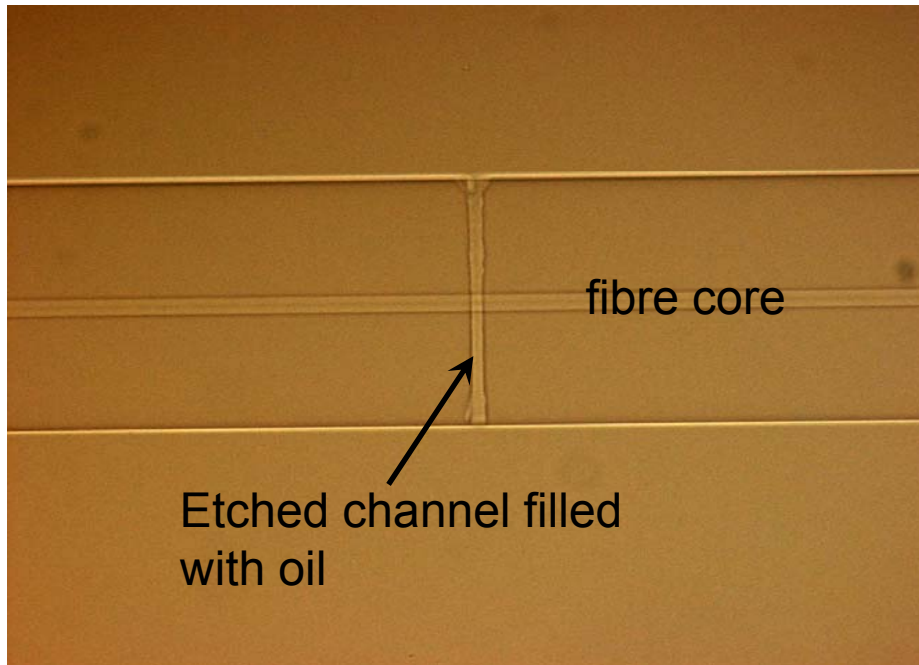
- ❑ Why femtosecond laser microprocessing?
- ❑ Modelling of femtosecond microfabrication
- ❑ Fiber-based photonic devices
 - Fibre Bragg Gratings
 - Long-Period Gratings
 - Short cavity Er:Yt fibre laser
- ❑ Planar structures
 - Waveguide fabrication
 - Sub-wavelength gratings
 - Experiments with high repetition rate system
- ❑ fs-assisted postprocessing (microfluidic applications)
- ❑ Future work

Femtosecond pulse laser inscription system setup



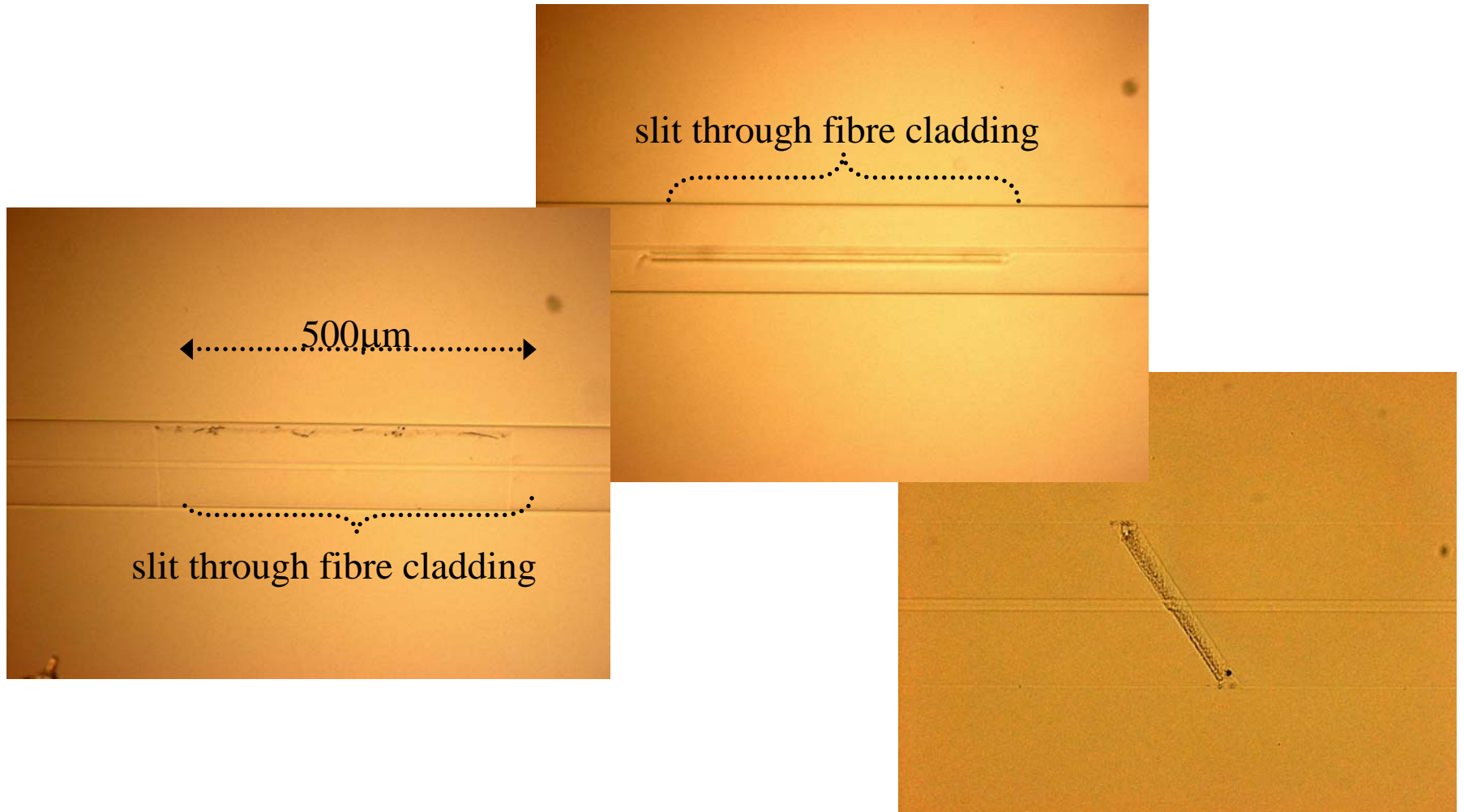
- ❑ Retain all aspects of fabrication setup except the inclusion of a conventional thin glass slip interface
- ❑ Less restrictive to fabrication dimensions

Fibre based microfluidic applications



- ❑ Application fields:
 - Microfluidic devices for biomedical analysis
 - Tunable micro-photonics devices
 - Fibre sensors
- ❑ Based on femtosecond laser pulse processing and selective chemical etching using hydrofluoric acid (HF)
 - Allows fabrication of arbitrary 2-D/3-D structures (defined by the moving laser focus)
 - Alleviates issues relating to accurate alignment/seal between channels and optical waveguide
- ❑ Resultant devices take advantage of merits of optical fibre waveguide e.g low loss, remote light delivery+ detection etc.

Complex channels



Future directions

☐ New materials

- Glasses, including active
- Silicon
- Crystals

☐ Planar geometry e.g. films

☐ Advanced processing (fs modification, machining, preprocessing etc., postprocessing such as etching etc.)

☐ Detailed modeling (3D Maxwell + adequate plasma model)

Conclusions

- ❑ Methods of microfabrication of photonic structures in glasses/dielectrics by means of the controlled focused fs laser pulse are developed
- ❑ A range of photonic devices has been demonstrated in fibre and planar geometries
- ❑ Adaptive high resolution high performance numerical modelling of fs inscription is undertaken
- ❑ Still a lot of things to do